

Woods Hole Oceanographic Institution



The Northwest Tropical Atlantic Station (NTAS): NTAS-4 Mooring Turnaround Cruise Report

by

Albert J. Plueddemann, William M. Ostrom, Nancy R. Galbraith,
Paul R. Bouchard, Brian P. Hogue, Brandon R. Wasnewski and M. Alexander Walsh

Woods Hole Oceanographic Institution
Woods Hole, MA 02543

May 2006

Technical Report

Funding was provided by the National Oceanic and Atmospheric Administration
under Grant No. NA17RJ1223 and the Cooperative Institute for Climate and Ocean Research (CICOR).

Approved for public release; distribution unlimited.



Upper Ocean Processes Group
Woods Hole Oceanographic Institution
Woods Hole, MA 02543
UOP Technical Report 2006-04

WHOI-2006-09

UOP-2006-04

**The Northwest Tropical Atlantic Station (NTAS):
NTAS-4 Mooring Turnaround Cruise Report**

by

Albert J. Plueddemann, William M. Ostrom, Nancy R. Galbraith, Paul R. Bouchard,
Brian P. Hogue, Brandon R. Wasnewski, M. Alexander Walsh

May 2006

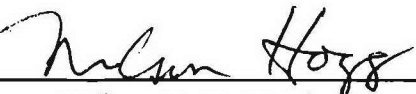
Technical Report

Funding was provided by the National Oceanic and Atmospheric Administration under Contract No. NA17RJ1223 and the Cooperative Institute for Climate and Ocean Research.

Reproduction in whole or in part is permitted for any purpose of the United States Government. This report should be cited as Woods Hole Oceanog. Inst. Tech. Rept., WHOI-2006-09.

Approved for public release; distribution unlimited.

Approved for Distribution:



Nelson G. Hogg, Chair

Department of Physical Oceanography

Abstract

The Northwest Tropical Atlantic Station (NTAS) was established to address the need for accurate air-sea flux estimates and upper ocean measurements in a region with strong sea surface temperature anomalies and the likelihood of significant local air-sea interaction on interannual to decadal timescales. The approach is to maintain a surface mooring outfitted for meteorological and oceanographic measurements at a site near 15°N, 51°W by successive mooring turnarounds. These observations will be used to investigate air-sea interaction processes related to climate variability.

Deployment of the first (NTAS-1), second (NTAS-2) and third (NTAS-3) moorings were documented in previous reports (Plueddemann et al., 2001; 2002; 2003). This report documents recovery of the NTAS-3 mooring and deployment of the NTAS-4 mooring at the same site. Both moorings used 3-meter discus buoys as the surface element. These buoys were outfitted with two Air-Sea Interaction Meteorology (ASIMET) systems. Each system measures, records, and transmits via Argos satellite the surface meteorological variables necessary to compute air-sea fluxes of heat, moisture and momentum. The upper 150 m of the mooring line were outfitted with oceanographic sensors for the measurement of temperature and velocity.

The mooring turnaround was done on the NOAA Ship *Ronald H. Brown*, Cruise RB-04-01, by the Upper Ocean Processes Group of the Woods Hole Oceanographic Institution. The cruise took place between 12 and 25 February 2004. The NTAS-3 buoy was found adrift and recovered on 19 February at 14°53.7'N, 51°22.8'W. Deployment of the NTAS-4 mooring was on 21 February at approximately 14°44.4'N, 50°56.0'W in 5038 m of water. A 30-hour intercomparison period followed, after which dragging operations to recover the lower portion of the NTAS-3 mooring commenced. This report describes these operations, as well as other work done on the cruise and some of the pre-cruise buoy preparations.

Table of Contents

Abstract	iii
List of Figures	v
List of Tables	vi
1. Introduction.....	1
2. Pre-Cruise Operations	2
a. Buoy Spins	4
b. Sensor Evaluation.....	6
3. NTAS-3 Mooring Recovery	8
a. Buoy Recovery	8
b. Dragging Operations	10
4. LIDEX Mooring Deployment	15
5. NTAS-4 Mooring Deployment.....	18
a. Mooring Design	18
b. Instrumentation	18
c. Deployment Operations	28
6. Meteorological Intercomparisons	31
a. Overview.....	31
b. NTAS-3 vs. <i>Ron Brown</i>	32
c. NTAS-4 vs. <i>Ron Brown</i>	36
7. CTD casts	40
 Acknowledgments.....	 42
References	42
Appendix 1. Cruise Participants	43
Appendix 2. Cruise Chronology	44
Appendix 3. NTAS-3 Moored Station Log	49
Appendix 4. NTAS-4 Moored Station Log	56
Appendix 5. Evaluation of NTAS-3 swage failure.....	62

List of Figures

Figure 1. NTAS site map.....	1
Figure 2. NTAS-4 cruise track.....	3
Figure 3. NTAS-4 WHOI buoy spin results	5
Figure 4. NTAS-4 Charleston buoy spin results	6
Figure 5. NTAS-4 wind speed evaluation	7
Figure 6. NTAS-3 buoy drift track	8
Figure 7. NTAS-3 buoy recovery	9
Figure 8. NTAS-3 swage failure	10
Figure 9. Dragging operation schematic	11
Figure 10. Dragging gear.....	12
Figure 11. Winch tension during dragging.....	14
Figure 12. LIDEX bathymetry survey.....	16
Figure 13. LIDEX mooring diagram	17
Figure 14. NTAS-4 mooring diagram	19
Figure 15. NTAS-4 mooring details.....	20
Figure 16. NTAS-4 tower top	21
Figure 17. NTAS-4 buoy well	22
Figure 18. NTAS-4 tower top layout	24
Figure 19. Aquadopp current meter	25
Figure 20. Workhorse ADCP.....	26
Figure 21. SBE-39 temperature sensor on load bar	27
Figure 22. SBE-39 temperature sensor in wire clamp	28
Figure 23. Tidbit temperature logger	28
Figure 24. Seabeam bathymetry at the NTAS site.....	39
Figure 25. Ship track during NTAS-4 deployment.....	30
Figure 26. NTAS-4 buoy deployment	31
Figure 27. Distance from NTAS-3 buoy	33
Figure 28. NTAS-3 vs. <i>Brown</i> : AT/RH	34
Figure 29. NTAS-3 vs. <i>Brown</i> : BP/PRC	34
Figure 30. NTAS-3 vs. <i>Brown</i> : SST/SSC	35
Figure 31. NTAS-3 vs. <i>Brown</i> : SWR/LWR.....	35
Figure 32. NTAS-3 vs. <i>Brown</i> : WND.....	36
Figure 33. NTAS-4 vs. <i>Brown</i> : AT/RH	38
Figure 34. NTAS-4 vs. <i>Brown</i> : BP/PRC.....	38
Figure 35. NTAS-4 vs. <i>Brown</i> : SST/SSC	39
Figure 36. NTAS-4 vs. <i>Brown</i> : SWR/LWR.....	49
Figure 37. NTAS-4 vs. <i>Brown</i> : WND.....	40
Figure 38. CTD profiles	41

List of Tables

Table 1. NTAS-4 WHOI buoy spin results	4
Table 2. NTAS-4 Charleston buoy spin results	5
Table 3. Winch payout vs. ship speed	13
Table 4. ASIMET sensor specifications	22
Table 5. NTAS-4 ASIMET serial numbers and sampling	23
Table 6. NTAS-4 sensor heights and separations	23
Table 7. NTAS-4 oceanographic sensor information	25
Table 8. NTAS-4 Aquadopp Configuration	26
Table 9. NTAS-4 ADCP Configuration.....	27

1. Introduction

The Northwest Tropical Atlantic Station (NTAS) project for air–sea flux measurement was conceived in order to investigate surface forcing and oceanographic response in a region of the tropical Atlantic with strong sea surface temperature (SST) anomalies and the likelihood of significant local air–sea interaction on interannual to decadal timescales. Two intrinsic modes of variability have been identified in the ocean–atmosphere system of the tropical Atlantic, a dynamic mode similar to the Pacific El Niño–Southern Oscillation (ENSO) and a thermodynamic mode characterized by changes in the cross-equatorial SST gradient. Forcing is presumed to be due to at least three factors: synoptic atmospheric variability, remote forcing from Pacific ENSO, and extra-tropical forcing from the North Atlantic Oscillation (NAO). Links among tropical SST variability, the NAO, and the meridional overturning circulation, as well as links between the two tropical modes, have been proposed. At present neither the forcing mechanisms nor links between modes of variability are well understood.

The primary scientific objectives of the NTAS project are to determine the in-situ fluxes of heat, moisture and momentum, to use these fluxes to make a regional assessment of flux components from numerical weather prediction models and satellites, and to determine the degree to which the oceanic budgets of heat and momentum are locally balanced. To accomplish these objectives, a surface mooring with sensors suitable for the determination of air–sea fluxes and upper ocean properties is being maintained at a site near 15°N, 51°W (Fig. 1) by means of annual “turnarounds” (recovery of one mooring and deployment of a new mooring at the same site).

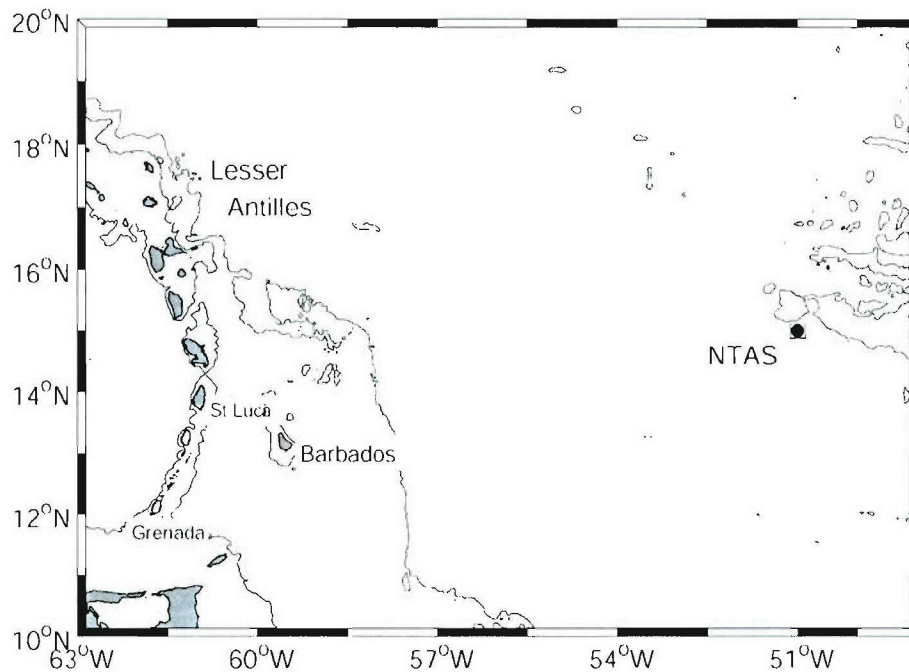


Figure 1. Location of the NTAS site (15 N, 51 W) with bathymetry at 1, 2, 3 and 4 km.

The surface elements of the moorings are 3-meter discus buoys outfitted with two complete Air–Sea Interaction Meteorology (ASIMET) systems. Each system measures, records, and transmits via Argos satellite the surface meteorological variables necessary to compute air–sea fluxes of heat, moisture and momentum. The upper 120–150 m of the mooring line is outfitted with oceanographic sensors for the measurement of temperature and velocity.

The NTAS-4 mooring turnaround was done on the NOAA Ship *Ronald H. Brown*, Cruise RB-04-01, by the Upper Ocean Processes Group (UOP) of the Woods Hole Oceanographic Institution (WHOI). The cruise was completed in 14 days, between 12 and 25 February 2004, and consisted of approximately 9 days of steaming, and 5 days of mooring operations. The cruise originated from Charleston, SC, and terminated in Bridgetown, Barbados, West Indies. The outbound leg was about 1900 nm (3520 km) from Charleston to the NTAS site, and the inbound leg was about 510 nm (945 km) from the NTAS site to Bridgetown (Fig. 2). The outbound leg was diverted slightly to the NE in order to pass by the Kiel Institut für Meereskunde (IFM) sound source mooring at 21°56.3'N, 62°34.2'W (an unsuccessful mooring recovery attempt was made there at the request of German researchers).

There were five principal operations during the cruise. First, the NTAS-3 buoy, which went adrift on 16 February due to a mooring component failure, was located and recovered. Second, a replacement Lagrangian Isopycnal Displacement Experiment (LIDEX) sound source mooring was deployed near 14°51'N, 51°14'W at the request of D. Hebert and T. Rossby of the University of Rhode Island. Third, the NTAS-4 mooring was deployed at 14°44.4'N, 50°56.0'W. The NTAS-4 deployment was followed by a 30-hour data intercomparison period, during which concurrent meteorological measurements from the NTAS-4 buoy and the ship were obtained. Finally, dragging operations were conducted in an attempt to retrieve the remainder of the NTAS-3 mooring.

This report consists of six main sections, describing pre-cruise operations (Sec. 2), the NTAS-3 mooring recovery (Sec. 3), the LIDEX mooring deployment (Sec. 4), the NTAS-4 mooring deployment (Sec. 5), meteorological intercomparisons (Sec. 6), and CTD casts (Sec. 7). Five appendices contain ancillary information.

2. Pre-Cruise Operations

Pre-cruise operations were conducted on the grounds of the US Coast Guard Vessel Support Facility in Charleston, SC. A shipment consisting of one 40' box truck and one flatbed truck left Woods Hole for Charleston on 3 Feb 2004. The box truck contained the buoy tower top, buoy and mooring instrumentation, science lab equipment, deck gear, and some mooring materials. Instrumentation and materials for deployment of a sound source mooring for the University of Rhode Island were also onboard. The flat bed truck transported a 20' "rag-top" container filled with mooring hardware and handling gear, a Tension Stringing Equipment (TSE) winch and three anchors.

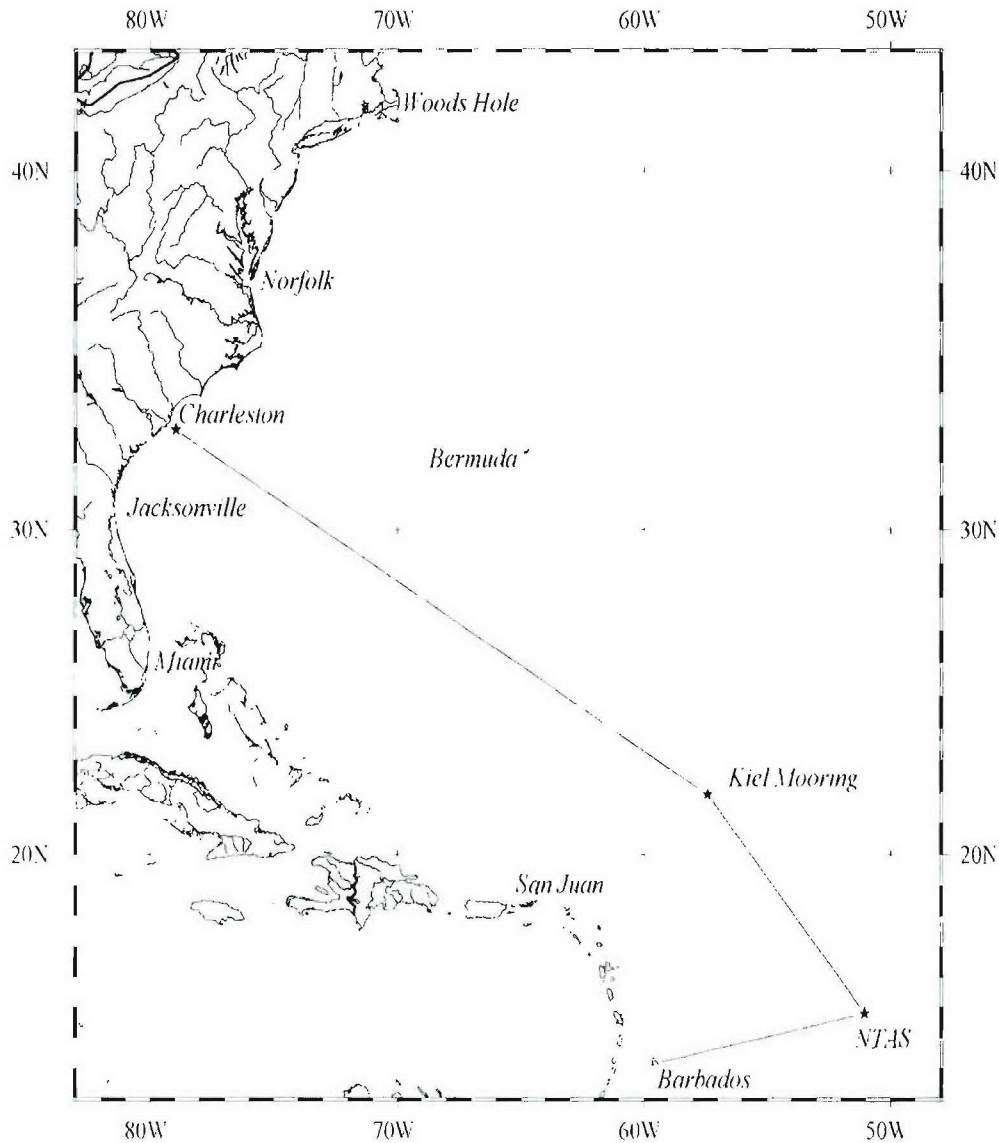


Figure 2. NTAS-4 cruise track, departing from Charleston, SC for the NTAS mooring site and returning to Bridgetown, Barbados. A stop was made near 22 N, 62.5 W to attempt recovery of a sound source mooring for IFM Kiel.

Two UOP representatives met the trucks in Charleston on 5 Feb and offloaded the gear directly onto the ship. An additional 5 people arrived in Charleston on 5 Feb for pre-cruise operations, which took place from 6-11 Feb. In addition to loading the ship, pre-cruise operations included assembly of the buoy well insert and tower top, a buoy spin, evaluation of ASIMET data, and preparation of the oceanographic instruments. The cruise chronology in Appendix 2 gives a more detailed breakdown of these activities.

a. Buoy Spins

A buoy spin begins by orienting the assembled buoy (without bridle legs attached) towards a distant point with a known (i.e., determined with a surveyor's compass) magnetic heading. The buoy is then rotated, using a fork-truck, through six positions in approximately 60-degree increments. At each position, the vanes of both wind sensors are oriented parallel with the sight line (vane towards the sighting point and propeller away) and held for several sample intervals. If the compass and vane are working properly, they should co-vary such that their sum (the wind direction) is equal to the sighting direction at each position (expected variability is plus or minus a few degrees).

The first buoy spins were done in the parking lot outside the WHOI Clark Laboratory high bay, with care taken to ensure that cars were not parked within about 30 ft of the buoy. The sighting angle to "the big tree" was about 309°. Both the buoy (with WND modules 215 and 216) and the spare tower top (WND module 214) were spun. The last compass, last vane, and direction (compass+vane) from test mode are reported below. Table 1 gives the sensor readings during the spins and Fig. 3 shows the direction results graphically.

Table 1. NTAS-4 WHOI buoy spin results

Position	Module SN	Last compass	Last vane	Compass + vane
1	214	122.0	182.9	304.9
	215	125.8	186.0	311.8
	216	120.2	188.1	308.2
2	214	303.8	2.3	306.1
	215	296.8	11.3	308.1
	216	302.3	5.2	307.5
3	214	192.5	114.4	306.9
	215	182.0	125.8	307.8
	216	180.5	127.0	307.5
4	214	72.1	239.9	312.0
	215	68.4	243.0	311.4
	216	67.1	247.5	314.6
5	214	11.2	300.3	311.5
	215	10.0	299.6	309.6
	216	8.2	305.4	313.6
6	214	247.5	60.6	307.1
	215	243.4	61.7	304.1
	216	245.4	65.4	310.8

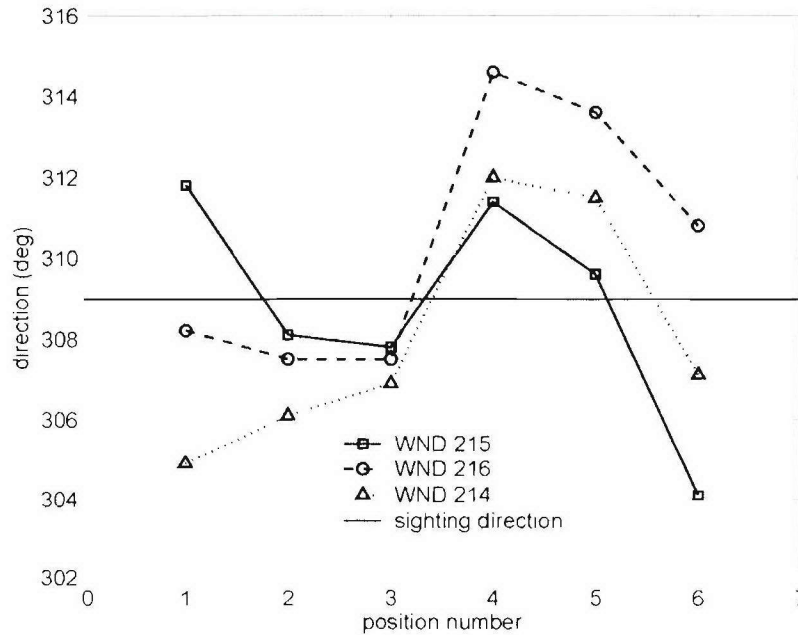


Figure 3. WHOI buoy spin results.

The second buoy spin was done in Charleston on an open area of pavement near the pier. A hand-held compass was used to determine that the magnetic field in the area was constant within a few degrees. A light pole approximately 1/2 mile away at a bearing of 29° was used as a sighting point. The technique used was the same as for the WHOI buoy spins. The last compass, last vane, and compass+vane from test mode are reported below. Table 2 gives the sensor readings during the spin and Fig. 4 shows the direction results graphically.

Table 2. NTAS-4 Charleston buoy spin results

Position	Module SN	Last compass	Last vane	Compass + vane
1	214	213.0	176.0	29.0
	216	204.9	183.9	27.8
2	214	269.3	117.9	27.2
	216	262.8	124.7	27.5
3	214	331.2	54.1	25.1
	216	324.5	62.4	26.9
4	214	30.7	3.2	33.9
	216	23.1	10.6	33.7
5	214	89.7	303.5	33.2
	216	83.3	311.1	34.4
6	214	149.2	241.5	28.7
	216	142.0	248.0	30.0

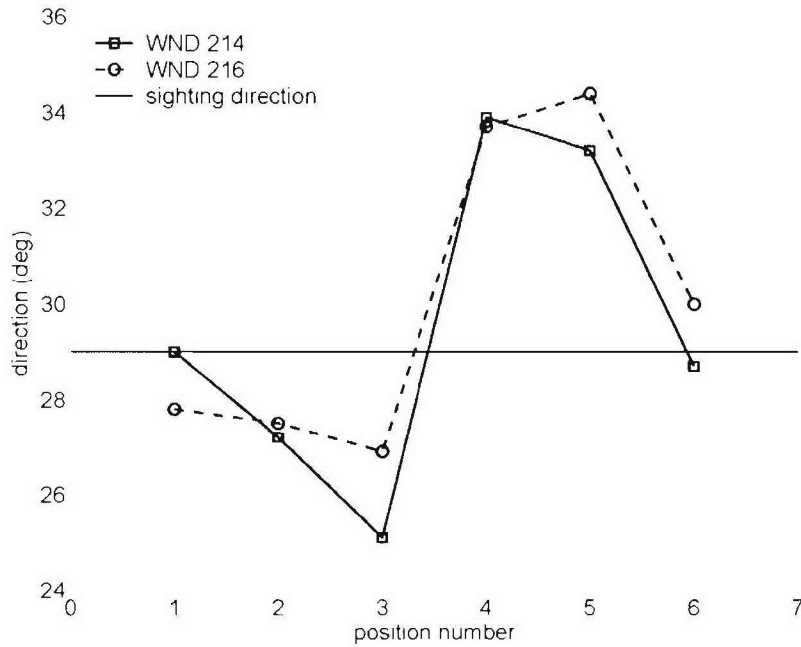


Figure 4. Charleston buoy spin results.

b. Sensor Evaluation

Once the buoy well-insert and tower top were assembled, the ASIMET modules were initialized, clamped to the tower and connected to the loggers. When mechanical assembly was complete, power was applied, the loggers were started, and data acquisition began. Evaluation of the primary sensor suite was done through a series of overnight tests. Both hourly Argos transmissions and 1 min logger data were evaluated.

On the morning of 8 February it was determined that both WND modules had failed during the previous night (Fig. 5). It was speculated that this was due to condensation inside the sensor housings as the ambient temperature dropped below 5°C overnight. Both units operated after being brought into the ship's lab. We decided to put fresh desiccant in the two failed instruments (WND 215 and 216) and run all three wind sensors simultaneously during the day. After finding that WND 215 (configured as a stand-alone unit during this test) failed to write to its flash card, we decided to leave WND 214 and 216 as the “primary” sensors on the buoy. We also requested and received two additional wind sensors from Woods Hole to be used as spares in case of another failure.

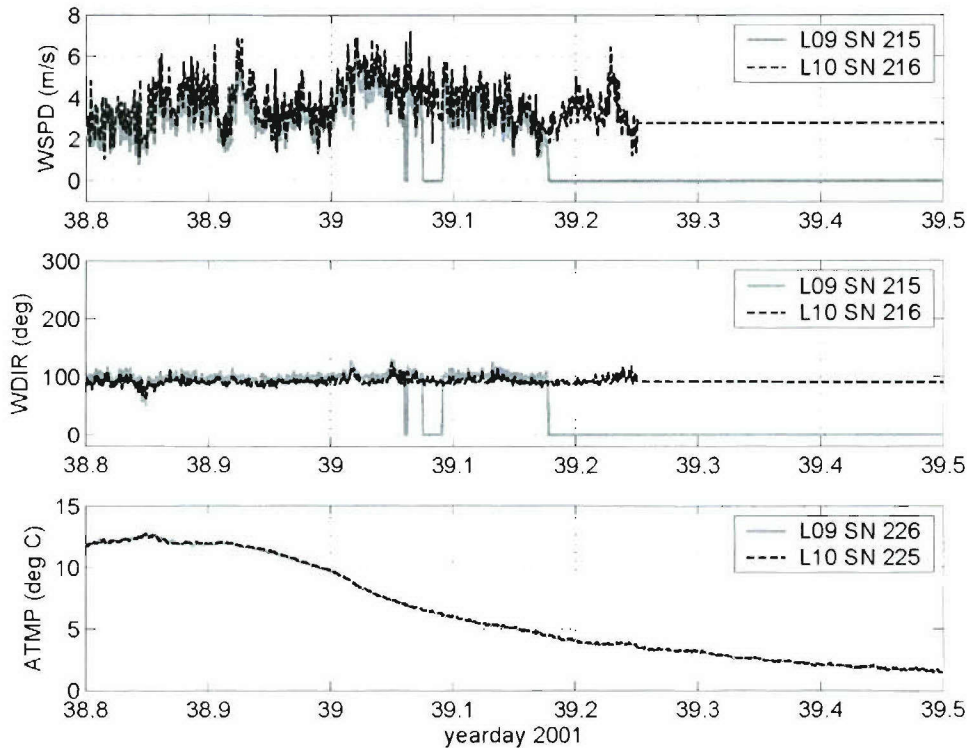


Figure 5. Time series of wind speed (upper) and direction (middle) from two wind modules, SN 215 and 216, on the buoy in Charleston. Both wind sensors failed as the air temperature (lower) dropped below 5 deg C.

Because the buoy was on the ship during the evaluation period, test conditions were degraded by air flow blockage and shading of radiation sensors during parts of the day. These problems were alleviated during a 16 hr period on 9-10 February when the buoy was placed on the dock with the “bow” to the wind and no notable flow obstructions. Evaluation of logger data from this period showed sensors performing as expected (differences between like sensors within accuracy tolerances) with the exception of longwave radiation. It was found that values from LWR 207 and 214 were in good agreement (difference $< 5 \text{ W/m}^2$) when the mean longwave radiation was near 250 W/m^2 . As mean longwave radiation increased to $\sim 400 \text{ W/m}^2$, LWR 214 read about 12 W/m^2 high compared to LWR 207. This behavior was not unexpected given the results of the pre-cruise calibrations done at WHOI (note that LWR 207 showed better agreement with the calibration standard). Given the typical range of longwave radiation values at the NTAS site ($380\text{-}460 \text{ W/m}^2$), we would expect LWR 214 to read $10\text{-}20 \text{ W/m}^2$ high.

A series of “sensor function checks,” including filling and draining the PRC modules, covering and uncovering the solar modules, and dunking the STC modules in a salt-water bucket, were done during the third day of in-port testing. The results of these checks, and a final in-port evaluation of hourly Argos data, showed all modules to be functioning as expected except for LWR biases, as noted above.

3. NTAS-3 Mooring Recovery

a. Buoy Recovery

En route to the NTAS operations site on 17 February, we received notification from UOP personnel monitoring Argos positions from WHOI that the NTAS-3 buoy showed several consecutive positions outside of its watch circle and was possibly adrift. An Iridium satellite telephone was used to send the most recent buoy positions to the ship from WHOI. The last position within the watch circle was at 1810 UTC on 15 February, after which the buoy showed a persistent drift to the NW at about 0.25 kt (Fig. 6). An estimate of the buoy position upon our arrival in the area was made based on the buoy drift speed, and the course of the *Brown* was adjusted in an attempt to intercept the buoy.

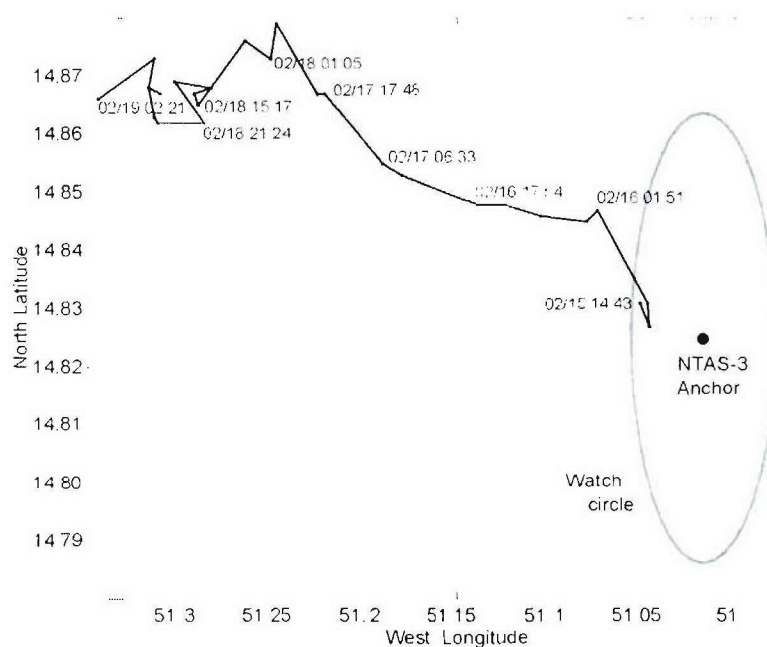


Figure 6. NTAS-3 buoy drift track after mooring component failure on 15 February. The buoy was recovered on 19 February.

The buoy was identified as a radar target at 1500 UTC on 19 February at a distance of about 9 nm, and was subsequently acquired visually. The ship maneuvered to within a few hundred feet of the buoy at 1600 UTC, and a position of 14°53.7'N, 51°22.8'W was obtained by hand-held GPS.

Recovery operations commenced in the same manner as described by Plueddemann et al. (2002), Sec. 6. The *Brown* maneuvered until the buoy was 10-15 m from the stern of the ship. The workboat was launched with two of the *Brown* deck crew and two UOP mooring technicians aboard. The workboat retrieved the pick-up hook, pole and line from the ship, attached the hauling line to the lifting bale on the buoy deck, and then returned to the ship. The A-frame was extended outboard as the line to the buoy was

hailed in, eventually causing the lifting bale to rotate towards the stern of the ship. The buoy was then lifted until the hull was about 1 m above the transom (Fig. 7), the A-frame was moved inboard, and tag lines were attached. With the buoy stabilized, the A-frame was shifted fully inboard and the buoy was lowered to the deck. The mooring line was disconnected from the buoy bridle and stopped-off, after which the buoy was shifted forward with the ship's crane and secured. The TSE winch line was attached to the mooring line and the mooring chain, instrumentation and wire rope were hauled in using the winch.

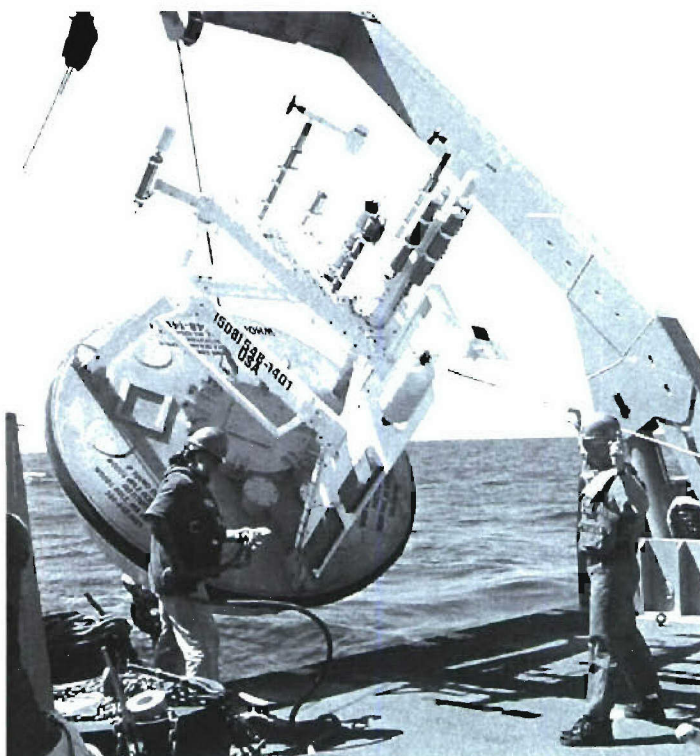


Figure 7. NTAS-3 buoy being lifted through the A-Frame (Photo by Wade Blake).

At the start of the mooring line recovery, it was unknown how much mooring material remained below the buoy. The uppermost instruments could be seen below the waterline, and the line was hanging nearly vertical, suggesting substantial weight below. In fact, the upper 600 m of the mooring, including all of the subsurface instrumentation, were recovered intact. The break in the mooring was found at the termination on the lower end of the first 500 m section of wire rope. The swage socket was fractured at the “shoulder” section, between the shank and the eye (Fig. 8).

The failed swage fitting was returned to WHOI for evaluation. Initial evaluation by WHOI engineers indicated a fatigue failure: The failure surface was smooth and contained a series of rings with increasing radius (“beach marks”). The fitting was then sent to the manufacturer, Crosby Inc., for further evaluation. Crosby’s report (Appendix 5) confirmed a fatigue failure, with a fracture initiated on one side below the eye and

propagating perpendicular to the plane of the eye. The beach marks indicated that the swage was subject to high-cycle, low-stress loading, as would be expected on a mooring with many wave cycles and most of the load carried longitudinally along the mooring line. There was no evidence of forging defects or improper swaging. The Crosby analysis suggested that the swage socket had been subjected to side-loading, which initiated the fracture.

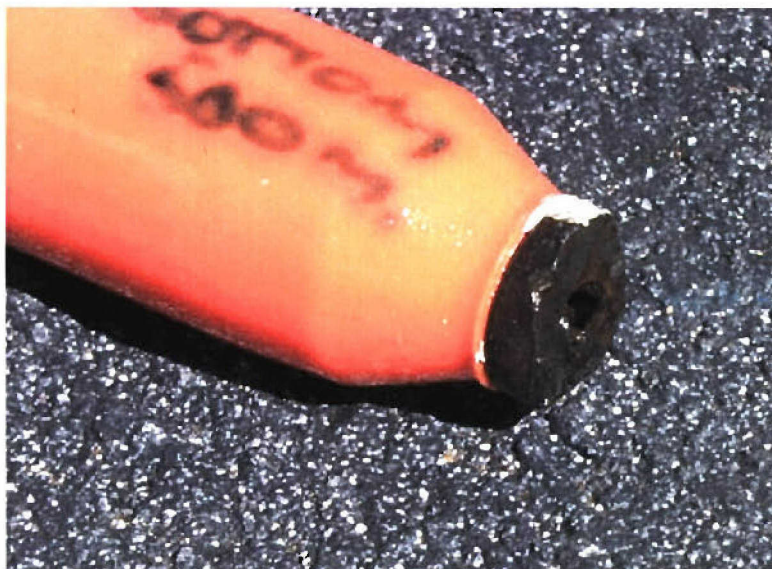


Figure 8. NTAS-3 swage failure. The boot and part of a swage fitting at the lower end of the first 500 m length of wire is shown.

b. Dragging Operations

The fact that only 600 m of the NTAS-3 mooring line was found attached to the buoy indicated that the majority of the mooring was still at the anchor site. Since the NTAS mooring was not designed with subsurface flotation sufficient to raise the mooring “bottom-first” to the surface, it was not possible to simply fire the release and recover the remainder of the mooring. Instead, the recovery mode was to hook the ship’s trawl-winch line to a portion of the mooring line by dragging specially designed grappling hooks along the sea floor. The UOP group brings a set of dragging gear on all mooring cruises for this purpose.

After recovering and completing all principal cruise activities, it was determined that sufficient time remained to attempt dragging operations. On 22 February the ship returned to the NTAS-3 anchor site and prepared dragging gear for attachment to the trawl winch line (Fig. 9-1). A 200 lb depressor weight was the lower-most element, followed by a 250 m wire leader and a second 200 lb depressor weight. The wire leader, part of the WHOI dragging gear, was used to avoid damage to the ship’s trawl wire. The upper portion of the wire leader was wound onto the TSE winch. Grappling hooks connected to short lengths of chain were attached at two points along the lower portion of

the leader, intended to hook the mooring line as the leader was dragged along the bottom. The depressor weights and hooks, prior to attachment to the wire, are shown in Fig. 10. The intention was to lay out 850 m of wire on the bottom prior to haul-back (Fig. 9-2). The UOP 12 kHz pinger was attached at 700 m above the upper depressor weight. This was intended to allow the altitude of the wire to be determined at the location of the pinger, and to ensure that the desired length of wire was in fact laid out along the bottom (i.e. when the pinger was at 100 m altitude). Unfortunately, it was not possible to track the pinger with the ship's echosounder, so instead wire was laid out until the signal from the pinger indicated that it was on its side.

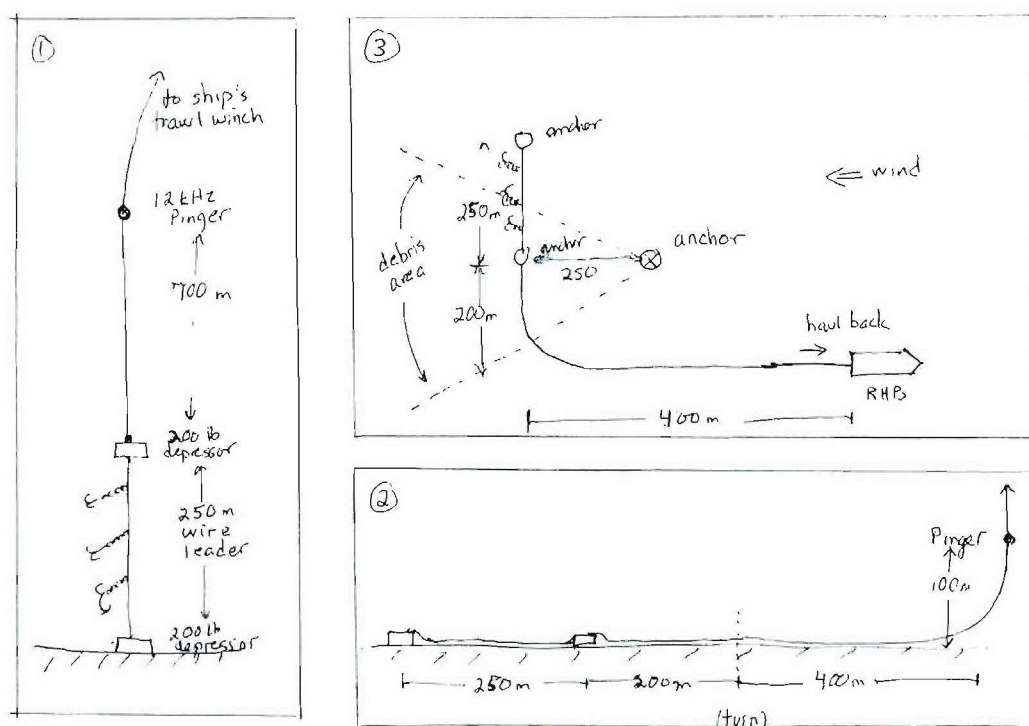


Figure 9. Concept sketch for dragging operations. Dragging gear is attached to the ship's trawl wire (1), the lower 850 m of wire is laid out on the sea floor as (2), as the ship maneuvers in an L-shaped pattern (3).

The scheme for dragging operations was determined based on knowledge of the release location and assumptions about the region where the mooring line would be found (Fig. 9-3). Argos buoy positions prior to the failure showed that the mooring was being stretched out towards the WNW relative to the anchor. Thus, it was assumed that the "debris field" would be found to the W of the anchor. In order to maximize the chance of hooking the mooring line, and minimize the amount of trawl wire needed, it was desirable to lay the dragging gear very close to the anchor. However, a wire angle of only a few degrees during payout could result in several hundred meters of horizontal offset at the seabed in 5000 m water depth. Thus, attempting to get too close could result in laying the wire on the wrong side of the anchor. It was decided that the target location for the lower depressor weight should be several hundred meters to the NW of the anchor. The

anchor position was well known ($14^{\circ}49.440'N$, $51^{\circ}01.254'W$ ± 20 m) based on a four-station acoustic survey of the release that was done prior to initiating dragging operations.

The initial scheme, as depicted in Fig. 9, called for dropping the lower depressor weight 350 m to the NW of the anchor and laying out the wire in an “L” shape about 450 m north-south by 400 m east-west. With the ship holding position at the SE corner of the “L,” the wire would be hauled back, dragging the hooks along the bottom and, hopefully, hooking into the mooring line. This operation was started about 1900 (local) on 22 February, but was suspended after about 1000 m of wire had been payed out due to the detection of smoke in the lower winch room. An electrical failure in the winch circuitry was found and eventually repaired. The winch was tested the following morning (1000 m of wire run out with a depressor weight as payload) and declared operational.

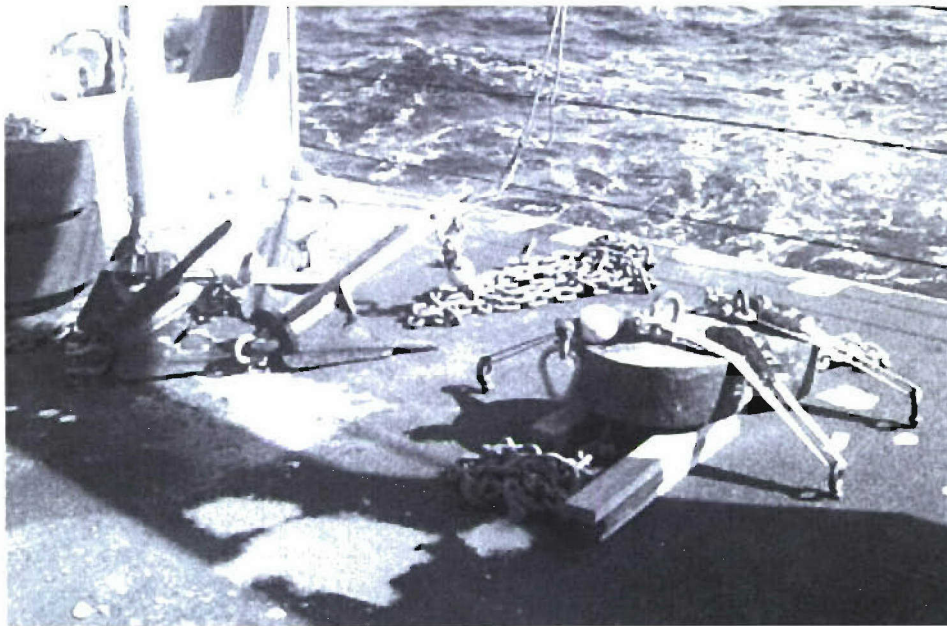


Figure 10. Dragging gear laid out on the fantail of the *Brown*.

Dragging operations began again at 1210 (local) on 23 February. The “L” shape was modified to be more conservative with respect to dropping the lower depressor too close to the anchor. The north-south distance from the anchor to the drop point was increased to 350 m, giving a range and bearing from the anchor of 430 m at 324° . The total north-south and east-west distances of the “L” were increased to 750 m (0.4 nm) and 650 m (0.35 nm) respectively. The pinger was relocated to 1150 m above the upper depressor weight to compensate for the increased wire to be payed out. At this location the pinger would be on the bottom (oriented horizontally) when the “L” was completely laid out.

Ship maneuvering for dragging was as follows. Initially, the ship held position at the starting point about 250 m west and 350 m north of the anchor. The dragging gear was deployed and the trawl winch payed out until the total wire out (winch wire counter

plus the leader length) slightly exceeded the water depth. At this point the lower depressor weight was on the bottom. Using dynamic positioning and autopilot, the *Brown* then began to “crab” to the south while maintaining the bow into the weather. While the ship crabbed southward at about 1 kt over a distance of about 0.4 nm, winch wire was payed out at 30-40 m/min. The ship’s speed was continuously monitored, and the payout speed adjusted, to ensure that the wire would be “pushed” to the seafloor rather than pulled away by the ship and lifted off the bottom. The values in Table 3 were used to adjust the payout speed to be about 20% greater than the ship’s speed through the water. Upon reaching the SW corner of the “L,” the ship steamed forward at about 1 kt while wire payout continued. Wire tension remained relatively steady at about 6000 lb during the wire payout (after the weights were on the bottom). The ship reached the stopping point for the payout (the SE end of the “L”) at about 1527 (local) with 6800 m of wire out, only about 6% more than would be expected if the wire angle were straight down in 5000 m of water and 1400 m were laid along the “L”.

Table 3. Winch Payout speed vs. ship speed

Ship Speed (kt)	Payout at (1:1) (m/min)	Payout at (1:1.2) (m/min)	Payout at (1:1.3) (m/min)	Payout at (1:1.4) (m/min)
0.10	3	4	4	4
0.20	6	7	8	9
0.25	8	9	10	11
0.30	9	11	12	13
0.40	12	15	16	17
0.50	15	19	20	22
0.60	19	22	24	26
0.70	22	26	28	30
0.75	23	28	30	32
0.80	25	30	32	35
0.90	28	33	36	39
1.00	31	37	40	43
1.10	34	41	44	48
1.20	37	44	48	52
1.25	39	46	50	54
1.30	40	48	52	56
1.40	43	52	56	61
1.50	46	56	60	65
1.60	49	59	64	69
1.70	52	63	68	73
1.75	54	65	70	76
1.80	56	67	72	78
1.90	59	70	76	82
2.00	62	74	80	86

recommended

Haul-back of the trawl wire began at 1533 (local; 2033 UTC) with the ship holding position at the SE end of the “L”. The wire was hauled back slowly (15 m/min) in order to avoid lifting the upper depressor weight off the bottom. The wire tension stayed relatively steady near 6000 lb for the first 2 h of haul back (Fig. 11). With 6550 m of wire out we established contact with the pinger, and the signal indicated that it was on its side. With 6160 m of wire out at 2120 UTC the pinger signal changed to indicate that it was oriented vertically. At this point, the wire initially laid out on the bottom was being lifted into the water column. The layout geometry indicates that if all of the trawl wire were lifted off of the bottom rather than being dragged, the upper depressor weight would be lifted (or dragged) when there was about 5800 m of wire out. No increase in tension was seen at this point, so it was assumed that the weights were dragged rather than lifted. By about 2230 UTC, with 4950 m of wire out, tension began to increase, indicating that the depressor weights were being lifted off of the bottom. This was consistent with the water depth near 5000 m in the area. The interpretation was that, despite no discernable increase in tension, the dragging gear had been pulled across the sea floor from a location NW of the anchor to almost directly beneath the ship before being lifted. This was the desired result.

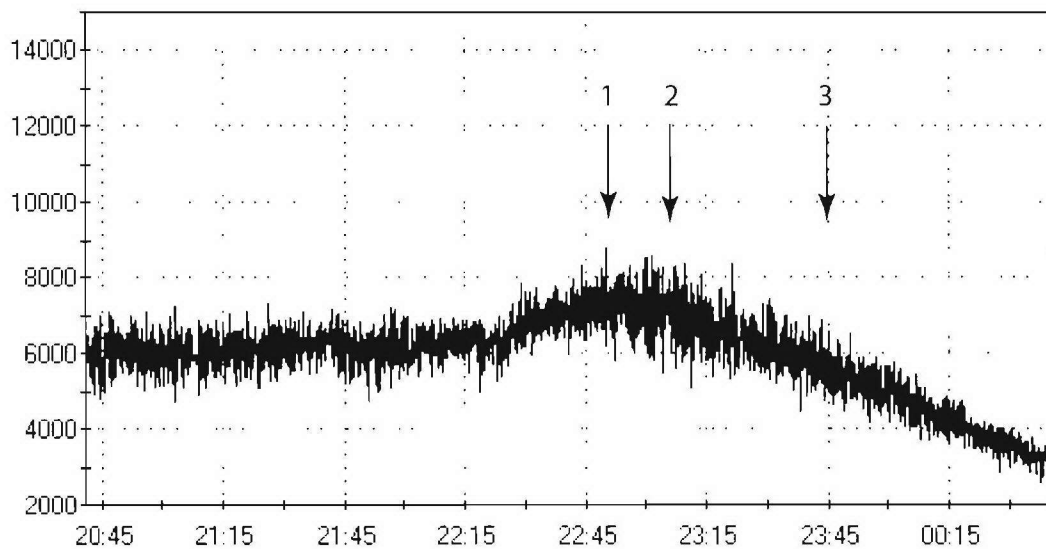


Figure 11. Trawl winch tension vs. time during dragging operations, starting about 15 min after wire haul-back. Arrows indicate approximate times when (1) dragging weights were off the bottom, (2) release was fired and (3) release was at its minimum slant range.

The lack of tension increase prior to the weights being lifted from the bottom meant that we did not have a “hard” hook into the anchor or a portion of the mooring line that was pulling directly on the anchor. However, with thousands of meters of mooring line on the bottom, it was conceivable that the line had been hooked, and slack was being pulled towards the ship without pulling against the anchor. It was also possible that wire rope or synthetic mooring line was slipping through a hook without “catching” on a termination (of course a third possibility was that the attempt to hook the mooring had failed).

The increasing tension near 2200 UTC convinced us that the mooring line had been hooked, and was beginning to tighten up against the anchor. The fear was that if we continued to haul against the line as it tightened, it would chafe and eventually break (particularly if it was the synthetic that had been hooked). After some discussion, it was decided that tension on the line could be reduced by firing the release, while at the same time having the ship steam forward to minimize the chance of the line going completely slack and falling away from the hook. The release was fired at 2310 UTC. Immediately afterwards the haul-back rate was increased from 15 m/min to 30 m/min and the ship steamed ahead to the E at about 1 kt. Wire tension began to drop soon afterwards, and ranging on the release showed its slant range to be decreasing. There was hope that the dragging operation had succeeded. However, by 2350 UTC slant range to the release began to increase, until it was falling away from the ship at a rate that approximately matched the speed of the ship through the water. It appeared that, if the mooring line ever had been hooked, we had lost it.

Dragging operations ended after about 8.5 h of work at about 2035 local on 23 Feb. When the lower depressor weight was hauled on deck with no sign of the mooring line anywhere on the dragging gear it was clear that the dragging had not been successful.

The final task prior to leaving the NTAS-3 site was to triangulate the release position. Simulation of an “upside down,” subsurface mooring, with a release and 8 glass balls at the top and 1400 m of wire at the bottom as an anchor, indicated that the polypropylene, and most of the nylon would be raised off the bottom, leaving the release hovering at about 1500 m depth. By using a corrected soundspeed of 1520 m/s, obtaining accurate slant ranges from three points, and then adjusting the depth until the three range circles intersected, it was possible to estimate both the location and depth of the release. This method resulted in a position of 14°49.80'N, 51°01.75'W, about 1.1 km NW of the anchor, and a depth of 1050 m.

4. LIDEX Mooring Deployment

The goal of the Lagrangian Isopycnal Dispersion Experiment (LIDEX), funded by the National Science Foundation, was to determine the processes that mix the waters in the tropical Atlantic horizontally (along constant density surfaces) and at what rate. As a part of this experiment, isopycnal RAFOS floats were deployed south of the Cape Verde Islands, off the coast of Africa, in 2003. The time of arrival of acoustic signals from sound source moorings allow the position of the floats to be determined. Four such source moorings were deployed at the start of LIDEX, but all four failed prematurely. At the request of Drs. Rossby and Hebert of URI, a supplemental sound source mooring was deployed on the NTAS-4 cruise.

The suggested site for the LIDEX mooring was a convenient spot within about 20 nm of the NTAS site with water depth near 5000 m. The Smith and Sandwell (1997) bathymetry for the region (Plueddemann et al., 2002, Fig. 14) indicated that the most

likely region would be to the NW of NTAS. An “L” shaped SeaBeam bottom survey grid covering about 70 nm² was laid out prior to the cruise. However, since the SeaBeam unit was found not to be operational, the 12 kHz echosounder was used to cover approximately the same area using a “radiator” pattern. The resulting bottom contours (Fig. 12) showed a suitable site at about 14°51.00'N, 51°14.40'W.

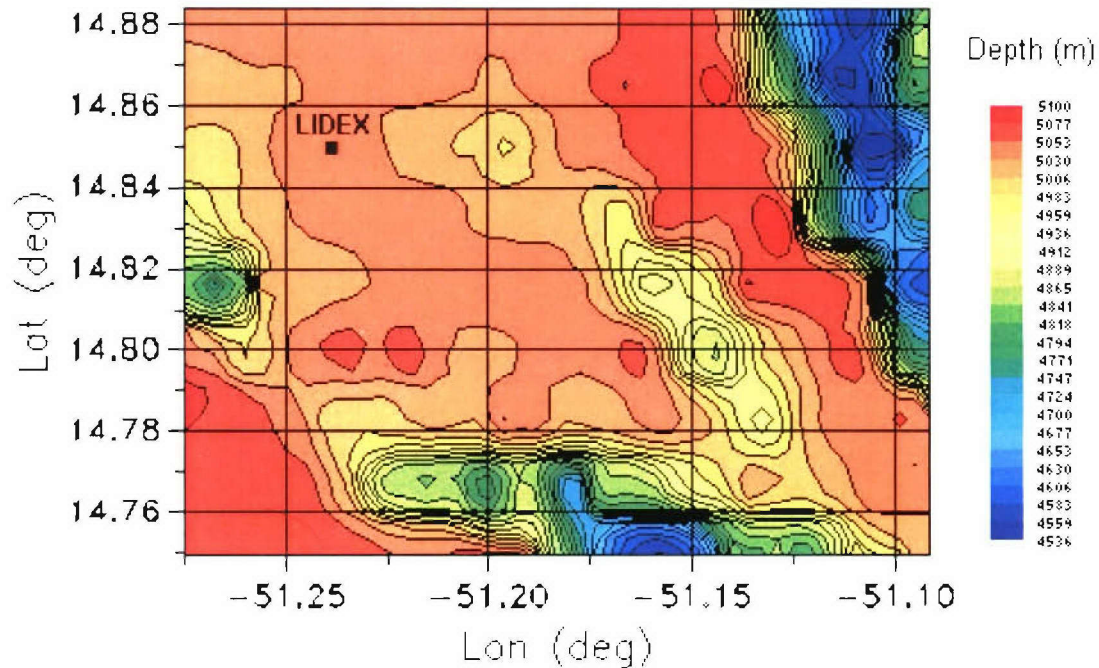


Figure 12. Bathymetry contour plot from the LIDEX echosounder survey, with the mooring location marked.

The LIDEX subsurface mooring was designed with twenty-four 17” glass balls for flotation, followed by 50 m of wire rope, the sound source electronics, and the sound source (Fig. 13). The lower portion of the mooring was made up of wire rope and synthetic. For water depth of 5000 m the sound source would be at the design depth of 1000 m. According to Dr. Hebert, the tolerance for the source location was a few hundred meters. However, since the actual water depth at the sight was known to be near 5070 m, one 50 m section of wire rope was added in the lower section of the mooring to more nearly match the depth of the sound source to the target depth. Following instructions provided by URI personnel, the sound source was turned on and proper operation was confirmed prior to deployment.

Deployment of the LIDEX mooring started on 20 February at 0800 (local) and took about 4 hours. The anchor drop was at 1658 UTC at a position of 14°50.983'N, 51°14.143'W and bottom depth of 5068 m. Since the mooring did not contain a release, it was not possible to triangulate the actual anchor position.

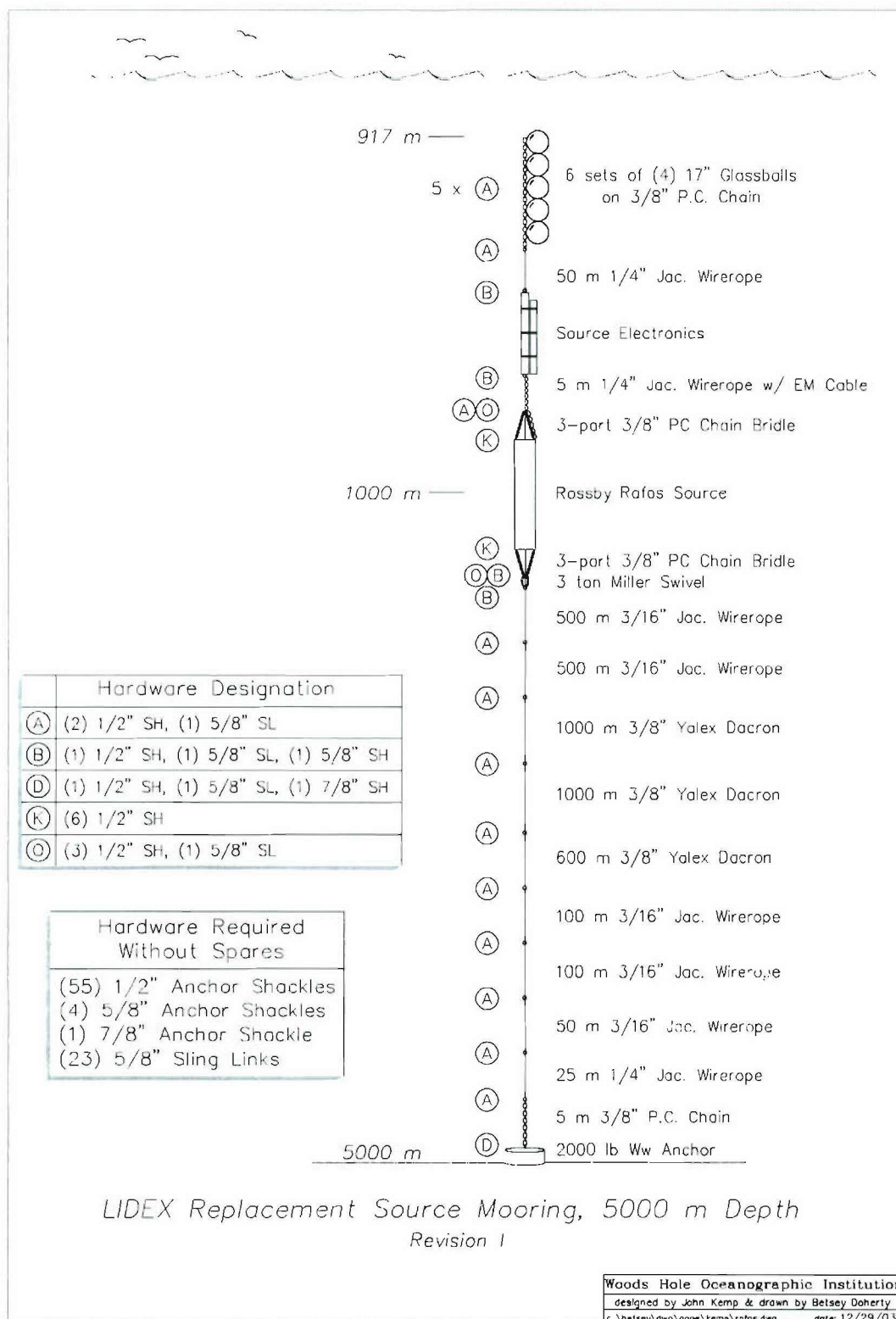


Figure 13. LIDEX mooring diagram.

5. NTAS-4 Mooring Deployment

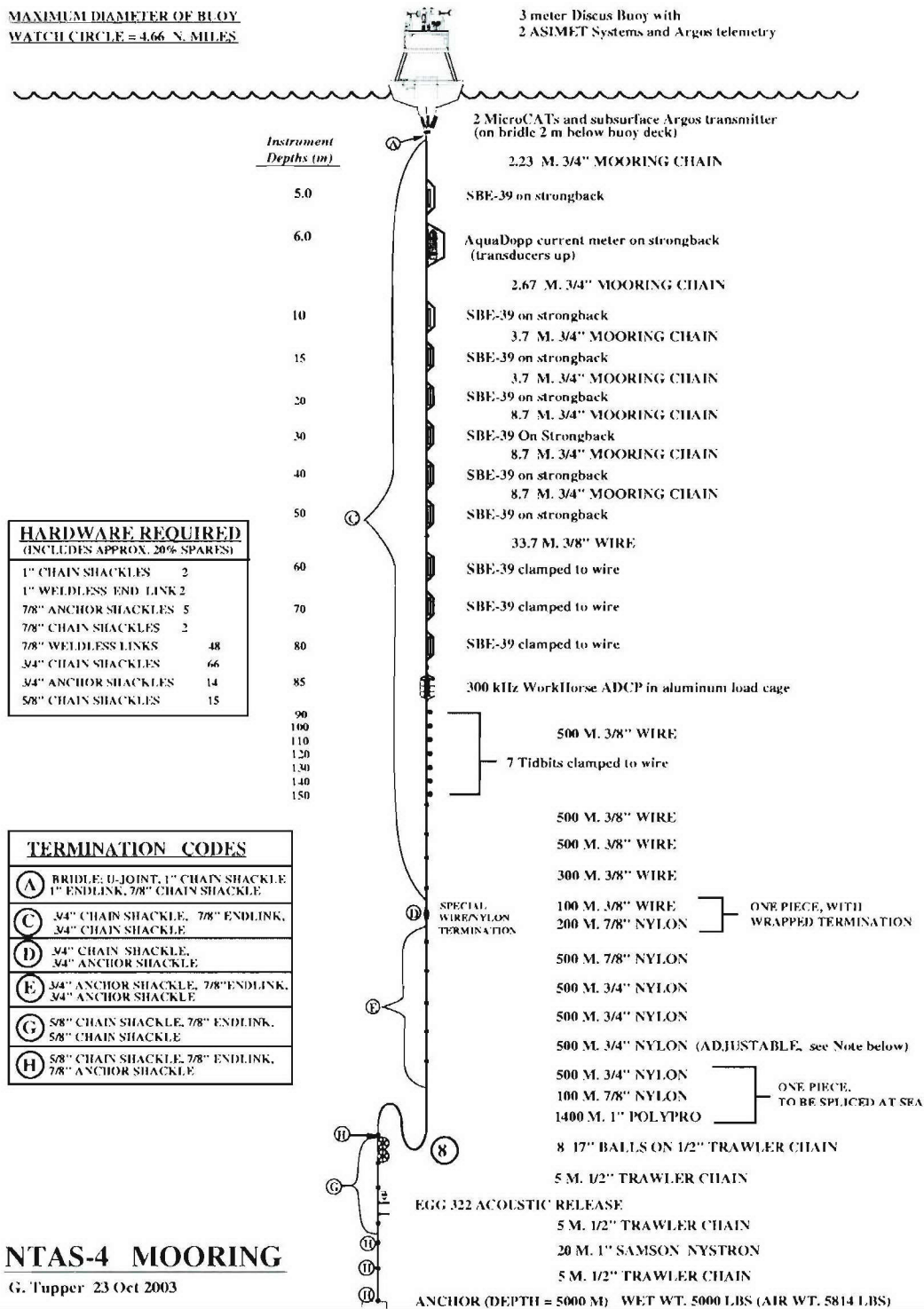
a. Mooring Design

The mooring is an inverse-catenary design of compound construction, utilizing chain, wire rope, nylon and polypropylene (Fig. 14). The mooring scope (ratio of total mooring length to water depth) is about 1.25. The watch circle has a radius of approximately 2.3 nm (4.3 km). The surface buoy is a 3-meter discus with a foam-filled aluminum hull providing approximately 10,000 lb of buoyancy. The buoy has a water-tight center well that houses two ASIMET data loggers and up to thirty-seven 120 Ah battery packs in a custom-made well insert. Two junction boxes and 12 ASIMET sensor modules are bolted to an aluminum tower that is approximately 3 m above the sea surface. The tower also contains a radar reflector, a marine lantern, and two independent Argos satellite transmission systems that provide continuous monitoring of buoy position. A third Argos positioning system, attached to a buoy bridle leg, is used as a backup and would be activated only if the buoy were to capsize. Sea surface temperature and salinity are measured by sensors bolted to the bridle legs and cabled to the loggers through a bottom access plate in the buoy well. Seventeen temperature sensors and two current meters are attached along the mooring using a combination of load cages (attached in-line between chain sections) and specially designed brackets (clamped along wire rope sections). All instrumentation is along the upper 150 m of the mooring line (Fig. 15). An acoustic release is placed approximately 30 m above the anchor. Above the release are eight 17" glass balls meant to keep the release upright and ensure separation from the anchor after the release is fired. This flotation is not meant for backup recovery; the buoyancy is not sufficient to raise the lower end of the mooring to the surface.

b. Instrumentation

The discus buoy was outfitted with two independent ASIMET systems to provide redundancy. The ASIMET system is the second-generation of the Improved Meteorological (IMET) system described by Hosom et al. (1995). Performance of the second-generation sensors is described by Colbo and Weller (submitted). The basic concept is a set of sensor modules that are connected to a central data logger and addressed serially using the RS485 communication protocol. As configured for NTAS-4, each system included six ASIMET modules mounted to the tower top (Fig. 16), one Sea-Bird SBE-37 "MicroCAT" mounted on the buoy bridle leg, a data logger mounted in the buoy well (Fig. 17), and an Argos Platform Transmit Terminal (PTT) mounted inside the logger electronics housing. The seven-module set measures ten meteorological and oceanographic variables (Table 4). Variables measured by the tower-top ASIMET modules are wind speed and direction (WND), barometric pressure (BPR), relative humidity and air temperature (HRH), shortwave radiation (SWR), longwave radiation (LWR), and precipitation (PRC). The MicroCAT measures sea temperature and conductivity (STC). The MicroCATs were specified with an RS485 interface option, and thus could be addressed by the ASIMET logger in the same manner as the meteorological modules on the tower top.

MAXIMUM DIAMETER OF BUOY
WATCH CIRCLE = 4.66 N. MILES



* Note: Unless water depth is more than 100 meters different than shown the length of this shot should remain 500 meters.

Figure 14. NTAS-4 mooring diagram.

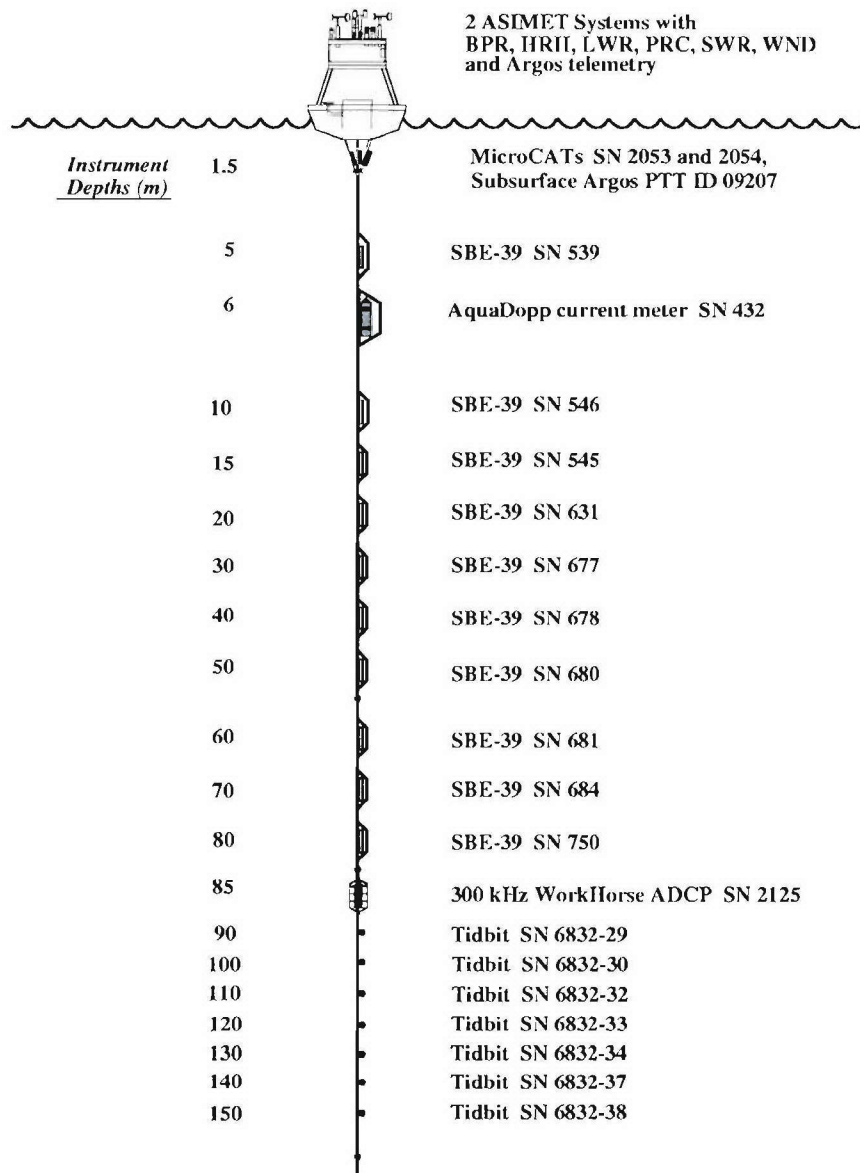


Figure 15. NTAS-4 mooring detail in the upper 150 m.

A wind vane on the tower top keeps the “bow” of the buoy oriented towards the wind. A marine lantern is mounted above the vane and flat-plate Argos PTT antennas are mounted on either side of the lower vane. The HRH modules are mounted on extension arms off the port and starboard bow to maximize aspiration and minimize self-heating. Wind modules are mounted in locations that minimize obstructions along the downwind path. Radiation sensors, mounted at the stern of the buoy, are at the highest elevation to eliminate shadowing.

A third Argos PTT, for position only (no data transmission) was added to the NTAS-4 buoy. This PTT (a Seimac SmartCAT) was intended as a backup to provide buoy position in the event that the two primary PTTs (Seimac WildCATs) failed. This precaution was considered necessary due to unexplained WildCAT PTT failures during the testing and deployment of other ASIMET systems. The position-only PTT was housed in a weatherproof case and mounted in the buoy well (Fig. 17). Four additional battery packs were mounted in the well insert to power the SmartCAT, and an additional flat-plate PTT antenna was mounted on the “starboard” side of the vane.

ASIMET sensor specifications are given in Table 4. Serial numbers of the sensors and loggers comprising the two systems (denoted ASIMET-1 and ASIMET-2) are given in Table 5. The sensor heights relative to the buoy deck, and relative to the water line, are given in Table 6. The water line was determined to be approximately 50 cm below the buoy deck by visual inspection after launch. The tower top sensor layout is shown graphically in Fig. 18.

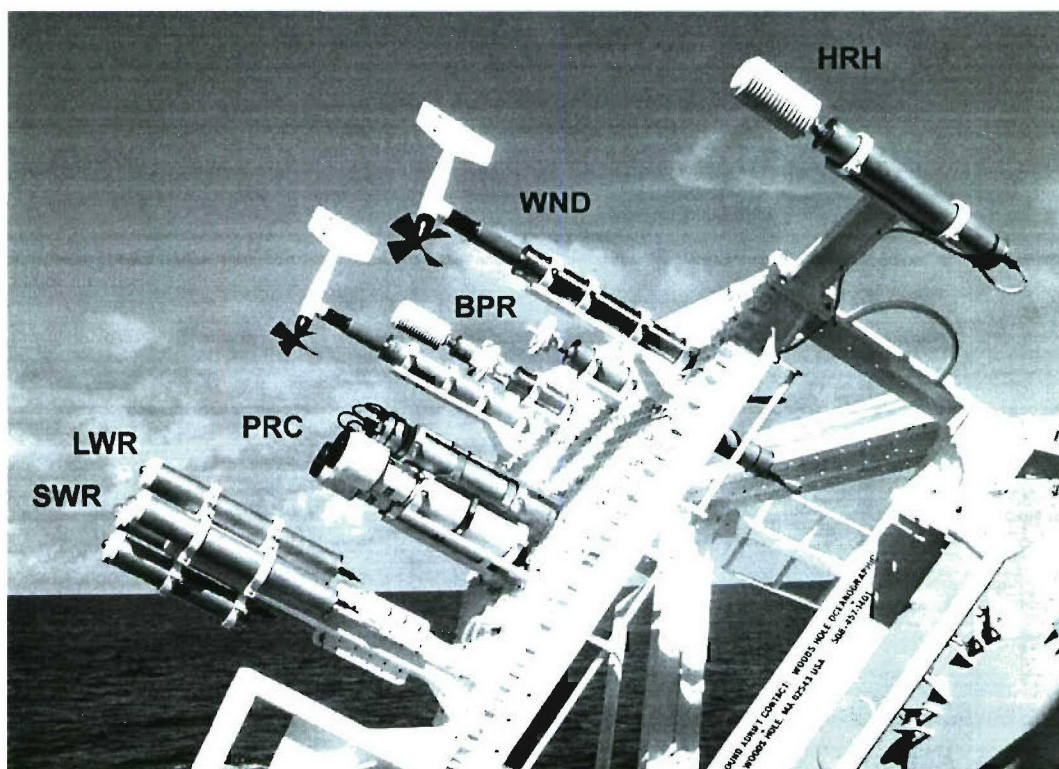


Figure 16. NTAS-4 tower top showing the location of ASIMET modules. The sea surface temperature and conductivity (STC) modules, located on the bridle legs, are not visible in this view.

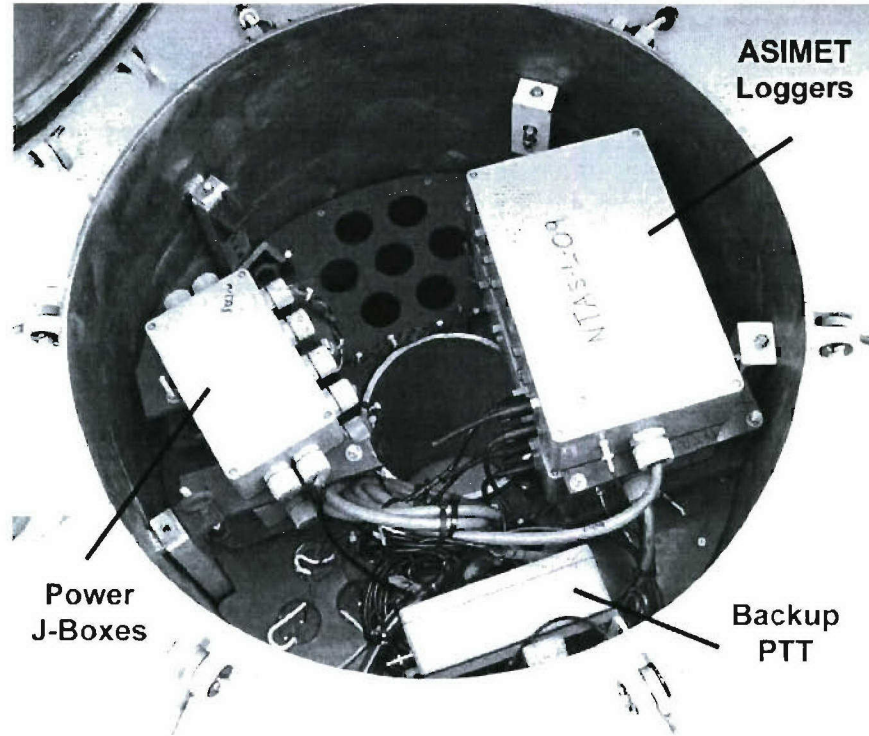


Figure 17. NTAS-4 buoy well showing the ASIMET data loggers and power junction boxes (two each, stacked vertically). Batteries are housed below the electronics platform.

Table 4. ASIMET sensor specifications

Module	Variable(s)	Sensor	Precision	Short-term Accuracy [1]	Long-term Accuracy [2]
BPR	barometric pressure	AIR Inc.	0.01 mb	0.3 mb	0.2 mb
HRH	relative humidity	Rotronic	0.01 %RH	3 %RH	1 %RH
	air temperature	Rotronic	0.02 °C	0.2 °C	0.1 °C
LWR	longwave radiation	Eppley PIR	0.1 W/m ²	8 W/m ²	4 W/m ²
PRC	precipitation	RM Young	0.1 mm	[3]	[3]
STC	sea temperature	SeaBird	0.1 m°C	0.1 °C	0.04 °C
	sea conductivity	SeaBird	0.01 mS/m	10 mS/m	5 mS/m
SWR	shortwave radiation	Eppley PSP	0.1 W/m ²	20 W/m ²	5 W/m ²
WND	wind speed	RM Young	0.002 m/s	2%	1%
	wind direction	RM Young	0.1 °	6 °	5 °

[1] Expected accuracy for 1 min values.

[2] Expected accuracy for annual mean values after post calibration.

[3] Field accuracy is not well established due to the effects of wind speed on catchment efficiency. Serra et al. (2001) estimate sensor noise at about 1 mm/hr for 1 min data.

Accuracy estimates are from Colbo and Weller (submitted) except conductivity, which is from Plueddemann (unpublished results).

Table 5. NTAS-4 ASIMET system serial numbers and sampling

System	Module	Type	Serial No.	Firmware Version [1]	Sample Rate [2]
ASIMET-1	BPR	ASIMET	202	VOS53 3.1	1 min
	HRH	ASIMET	226	VOS53 3.2	1 min
	LWR	ASIMET	207	VOS53 2.5	1 min
	PRC	ASIMET	211	VOS53 3.3	1 min
	STC	SBE-37	2053	SBE 2.2	5 min
	SWR	ASIMET	212	VOS53 3.3	1 min
	WND	ASIMET	214	VOS53 3.3	1 min
	Logger	C530/NTAS	L09	LGR53 2.7	1 min
	PTT	WildCAT	18112	ID#1 20741 ID#2 20892 ID#3 20898	90 sec 90 sec 90 sec
ASIMET-2	BPR	ASIMET	213	VOS53 3.1	1 min
	HRH	ASIMET	225	VOS53 3.2	1 min
	LWR	ASIMET	214	VOS53 3.5	1 min
	PRC	ASIMET	213	VOS53 3.3	1 min
	STC	SBE-37	2054	SBE 2.2	5 min
	SWR	ASIMET	214	VOS53 3.3	1 min
	WND	ASIMET	216	VOS53 3.5	1 min
	Logger	C530/NTAS	L10	LGR53 2.7	1 min
	PTT	WildCAT	18128	ID#1 20956 ID#2 20957 ID#3 20959	90 sec 90 sec 90 sec
Spare	PTT	SmartCAT	19486	ID#1 09207	110 sec

[1] For PTTs, Argos PTT ID is given rather than firmware revision.

[2] All modules sample internally. The logger samples all modules.

For PTTs, "sample rate" is the transmission interval.

Table 6. NTAS-4 ASIMET module heights and separations

Module	Relative [1] Height (cm)	Absolute [2] Height (cm)	Horizontal Sep. (cm)	Measurement Location
SWR	320	370	23	top of case
LWR	321	371	23	top of case
WND	293	343	116	middle of vane
PRC	262	312	19	top of cylinder
BPR	239	289	44	center of plate
HRH	240	290	253	center of shield
STC	-198	-148	32	center of shield

[1] Relative to buoy deck, positive upwards

[2] Relative to buoy water line, positive upwards

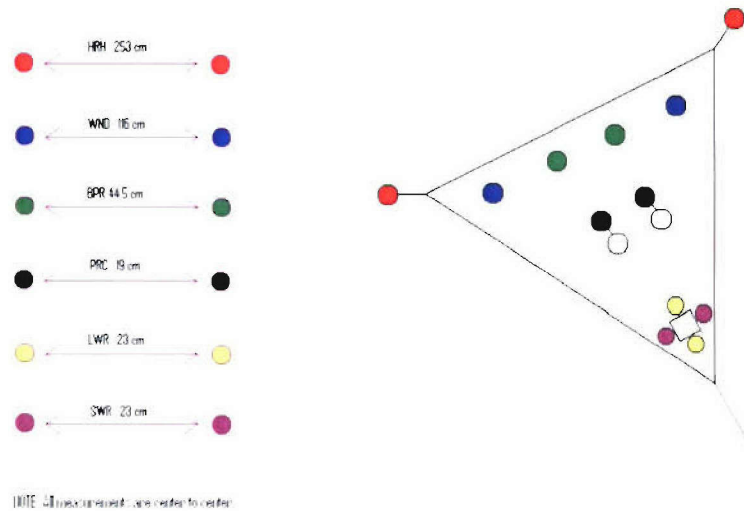


Figure 18. NTAS-4 tower top layout and module separations shown graphically.

Each tower-top module records one-minute data internally to a PCMCIA “flash” memory card at one-hour intervals. The STC module records internally at five-minute intervals. The logger polls each module during the first few seconds of each minute, and then goes into low-power mode for the rest of the minute. Further details of the sampling scheme are described in Plueddemann et al. (2001). The logger writes one-minute data to a flash memory card once per hour, and also assembles hourly averaged data for transmission through Argos PTTs. The Argos transmitter utilizes three PTT IDs to transmit the most recent six hours of one-hour averaged data.

A summary of the oceanographic sensor locations, serial numbers, and sample rates is given in Table 7. The description and specifications of individual sensors are the same as in Plueddemann et al. (2003). A brief description is provided here.

An Aquadopp current meter measuring three components of velocity along with temperature and pressure was deployed on the NTAS-4 mooring with the transducers at 6 m depth. A titanium load bar and bolt-on cage was used to attach the Aquadopp in-line between chain sections of the mooring (Fig. 19). The Aquadopp configuration parameters are given in Table 8. A priority was placed on resolving surface wave motion within each averaging interval. Evaluation of previous NTAS deployments indicated that the Aquadopp batteries were nearly depleted upon recovery. Thus, for NTAS-4 the measurement load (pings per second) was reduced from 22% to 17%. The configuration included the collection of diagnostic data (a short time series of 1-s samples) once per day. The predicted horizontal velocity precision was 0.4 cm/s.

Table 7. NTAS-4 Oceanographic sensor information

Depth (m)	Instrument	SN	Variable(s) measured [1]	Sample rate
5	SBE-39	539	T	5 min
6	Aquadop	432	T, V, P	60 min
10	SBE-39	546	T	5 min
15	SBE-39	545	T	5 min
20	SBE-39	631	T	5 min
30	SBE-39	677	T	5 min
40	SBE-39	678	T	5 min
50	SBE-39	680	T	5 min
60	SBE-39	681	T	5 min
70	SBE-39	684	T	5 min
80	SBE-39	750	T	5 min
85	ADCP	2125	T, V	60 min
90	Tidbit [2]	29	T	30 min
99	Tidbit	30	T	30 min
110	Tidbit	32	T	30 min
120	Tidbit	33	T	30 min
130	Tidbit	34	T	30 min
140	Tidbit	37	T	30 min
150	Tidbit	38	T	30 min

[1] T = temperature, V = velocity, P = pressure

[2] All Tidbit SNs begin with 6832 (e.g. 30 => 683230)

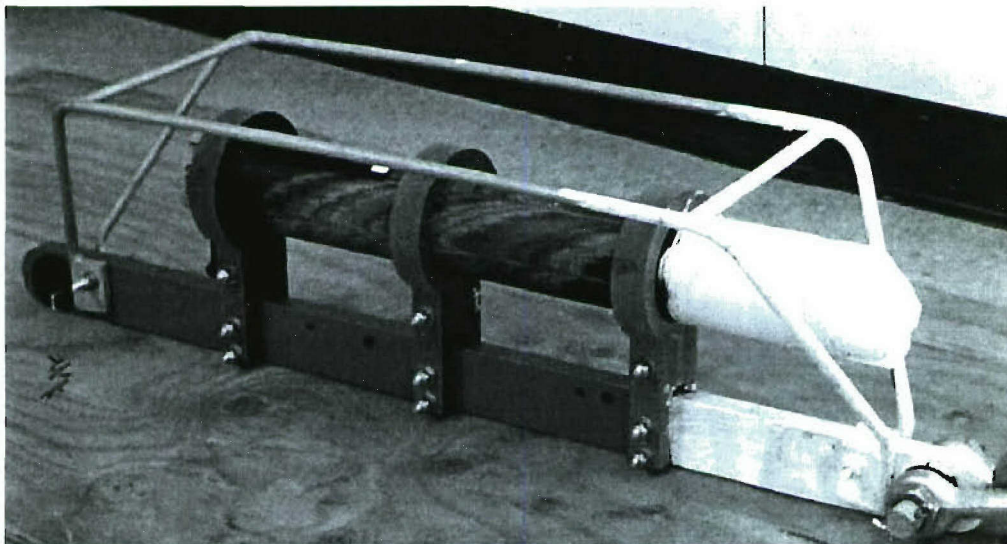


Figure 19. The Aquadop current meter attached to a titanium load bar and protected by a bolt-on cage. Anti-fouling paint has been applied to the upper portion of the assembly, including the transducer.

Table 8. NTAS-4 Aquadopp configuration

Parameter	Value	Units
Transmission interval	1	sec
Averaging interval	180	sec
Sample interval	60	min
Blanking Distance	1.0	m
Diagnostics interval	1440	min
Diagnostics samples	20	---
Measurement load	17	%
Power level	"HIGH-"	---
Compass update rate	1	sec
Coordinate system	ENU	---
Recorder Size	5	Mb

A 300 kHz RD Instruments Workhorse ADCP was deployed on the NTAS-4 mooring with the transducers at 85 m depth, facing upwards. The instrument was housed in a welded aluminum load cage (Fig. 20), and placed in-line between wire sections of the mooring. Details of the Workhorse configuration are given in Table 9. Results from previous NTAS deployments with the ADCP at 100 m depth had shown that the maximum range was about 85 m. Thus, for NTAS-4 the Workhorse was moved up to 85 m depth on the mooring. Due to side lobe reflections the maximum useable range is about 80 m (i.e., to within 5 m of the surface). The predicted velocity precision is 0.3 cm/s.

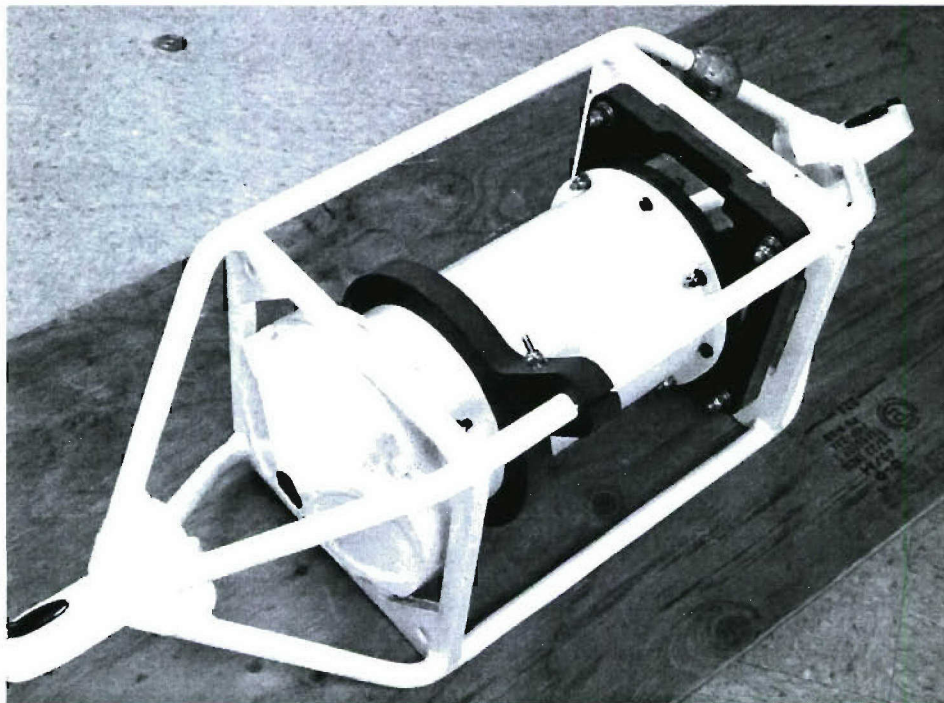


Figure 20. The 300-kHz ADCP in welded aluminum load cage. Anti-fouling paint has been applied to the ADCP transducer head.

Table 9. NTAS-4 ADCP configuration

Parameter	Value	Units
Time between pings	1	sec
Pings per ensemble	120	---
Ensemble interval	60	min
Number of depth bins	25	---
Depth bin length	4	m
Pulse length	4	m
Blank after transmit	3	m
Transducer orientation	up	---
Coordinate system	earth	---
Recorder Size	48	Mb

Ten Sea-Bird SBE-39s temperature sensors were attached to the mooring line using two different techniques. In the upper 50 m, where chain sections were used, seven instruments were clamped to titanium load bars (Fig. 21) and the load bars were then attached in-line using shackles and pear rings. The instrument spacing was 5 m in the upper 20 m, increasing to 10 m spacing below. Between 60 and 80 m three instruments were clamped directly to the wire using specially designed clamps (Fig. 22). These instruments had 10 m spacing. The instruments were power limited, with a minimum sample interval of 5 min for a one-year deployment.

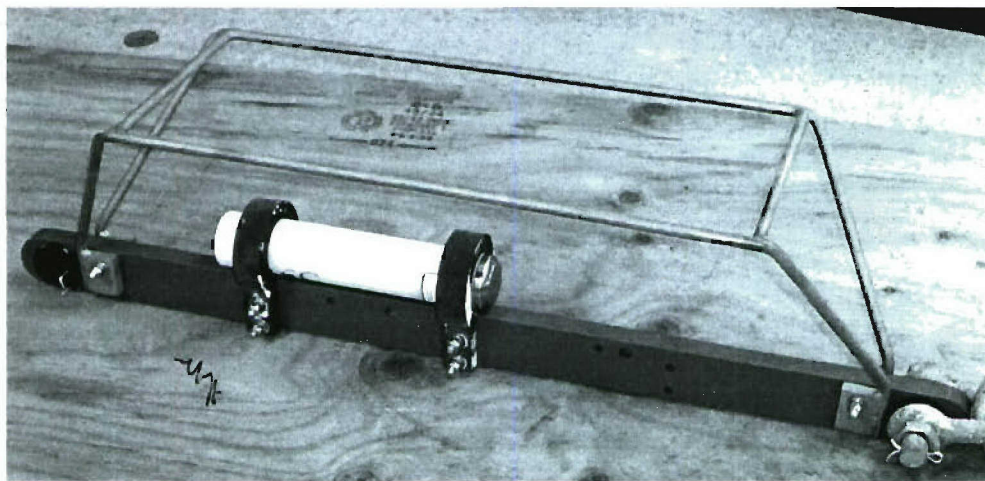


Figure 21. SBE-39 temperature sensor attached to a titanium load bar. Anti-fouling paint has been applied to the load bar.

Seven Onset Stowaway Tidbit temperature loggers were attached to the mooring wire at 10 m intervals between 90 and 150 m depth using specially designed brackets (Fig. 23). The minimum sampling interval appropriate for a 1-year deployment was 30 min (677 days duration).

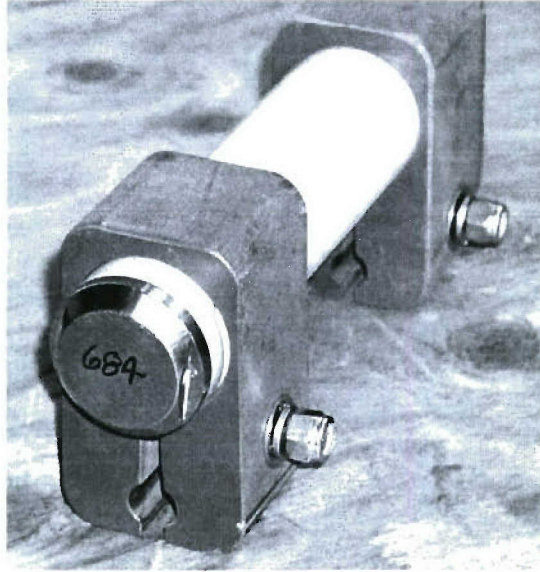


Figure 22. SBE-39 mounded in a wire clamp. No anti-fouling paint was applied.

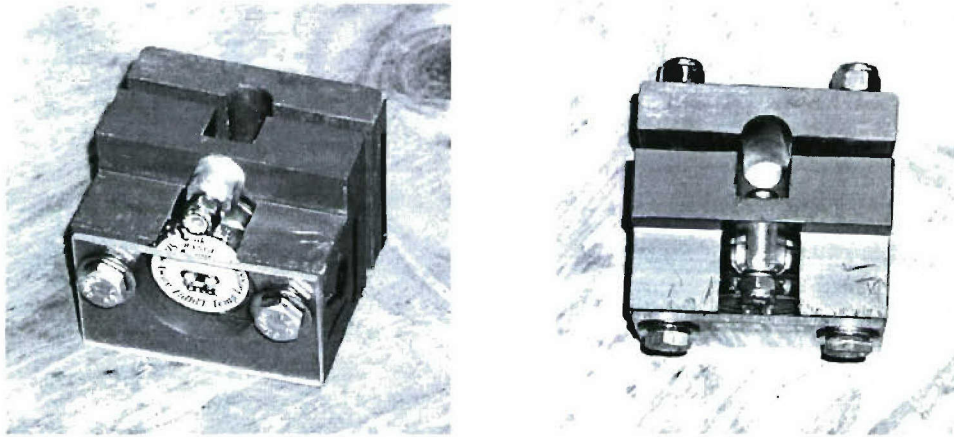


Figure 23. Tidbit temperature logger in plastic bracket used for attachment to wire. Front view (left) and top view (right) are shown.

c. Deployment Operations

The nominal NTAS deployment site is 15°N , 51°W , near the southwestern flank of Researcher Ridge. A SeaBeam bottom survey during the NTAS-2 cruise (Plueddemann et al., 2002) showed that there were two relatively flat regions within an area of approximately 200 nm^2 (700 km^2) centered at $14^{\circ}46'\text{N}$, $50^{\circ}58'\text{W}$. The first area, near $14^{\circ}50'\text{N}$, $51^{\circ}01'\text{W}$, showed depths of $4980 \text{ m} \pm 60 \text{ m}$ and was the anchor site for NTAS-1 and NTAS-3. The second area, near $14^{\circ}45'\text{N}$, $50^{\circ}56'\text{W}$, showed depths of $5040 \text{ m} \pm 50 \text{ m}$. This was the anchor site for NTAS-2, and was to be re-occupied by NTAS-4. The target NTAS-4 anchor drop site was chosen as $14^{\circ}44.50'\text{N}$, $50^{\circ}56.00'\text{W}$, about 7 nm (13 km) to the southeast of the NTAS-3 anchor (Fig. 24).

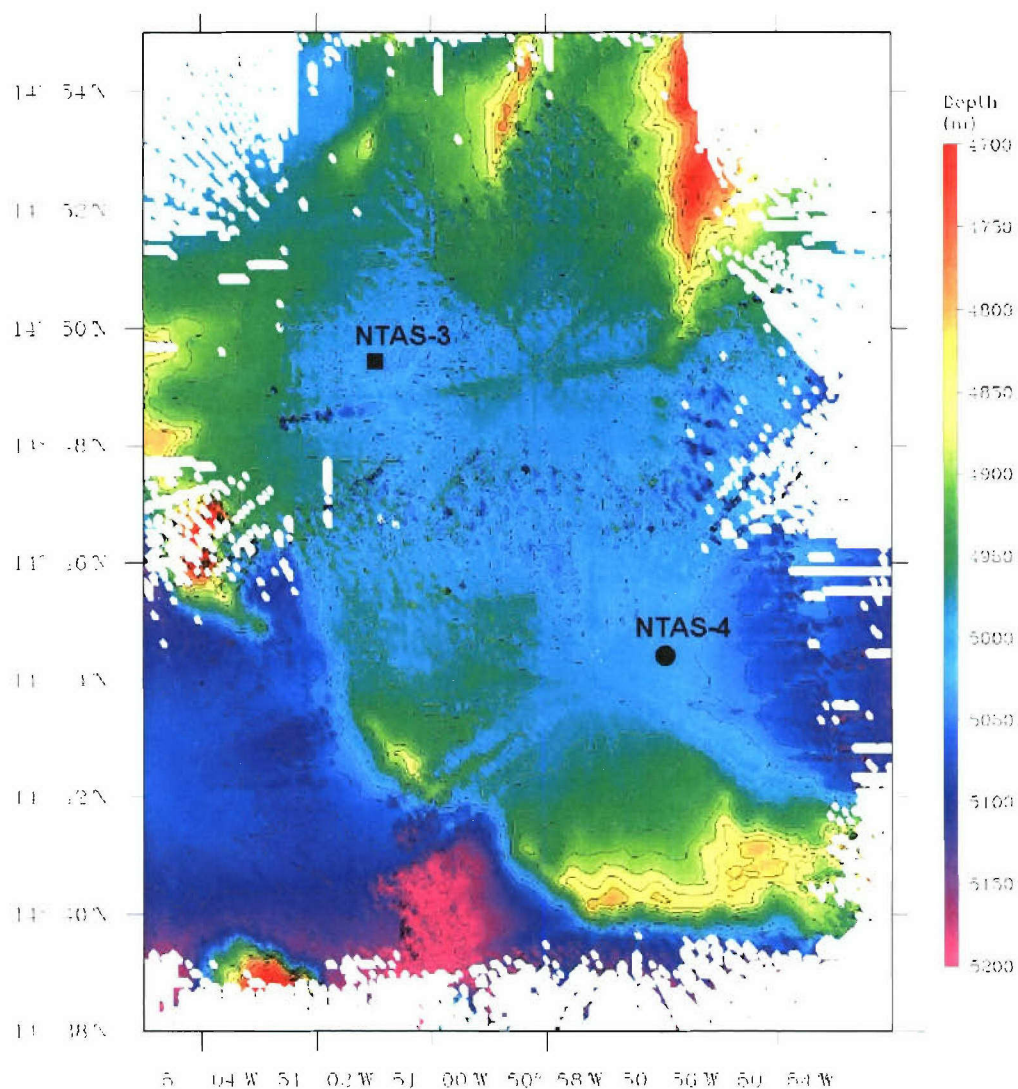


Figure 24. SeaBeam bathymetry at the NTAS site. The approximate NTAS-3 (square) and NTAS-4 (circle) anchor positions are shown.

Winds from the shipboard IMET system and currents from the shipboard ADCP were noted while maneuvering to NTAS-4 deployment starting point. Winds were relatively steady at 8-10 kt from the E, and currents were 10-15 cm/s to the SE. It appeared that the best approach would be from nearly due W of the anchor drop site. It was decided to steam to a starting point approximately 4.5 nm W of the drop site and hold position to set up for deployment operations.

Deployment operations began at about 1700 h (local) on 20 February with the *Brown* at a distance of 4.7 nm from the drop site (Fig. 25). The deployment scenario was nearly identical to that described by Plueddemann et al. (2002) for the NTAS-2 mooring,

and is not described in detail here. The upper 40 m of the mooring (chain and instruments) were deployed first with the ship hove to. At 1745 h the 3-meter discus buoy was deployed from the port side (Fig. 26) and brought around behind the ship. The remainder of the mooring was payed out as the ship made way at about 1 kt over the ground towards the drop site. At 2150 h local the mooring was completely in the water except for the anchor, and was under tow with the ship about 0.4 nm from the drop site. The anchor was dropped at 2216 h local on 20 February (21 February 0316 UTC) at 14°44.46'N, 50°55.74'W in water of depth 5048 m. Immediately following the anchor drop, the ship steamed about 0.25 nm to the S and hove to in order to track the buoy moving towards the ship on radar. By 2315 h the buoy appeared to have settled out, and the intercomparison period began. The anchor survey was delayed until after the intercomparison was completed on 22 February.

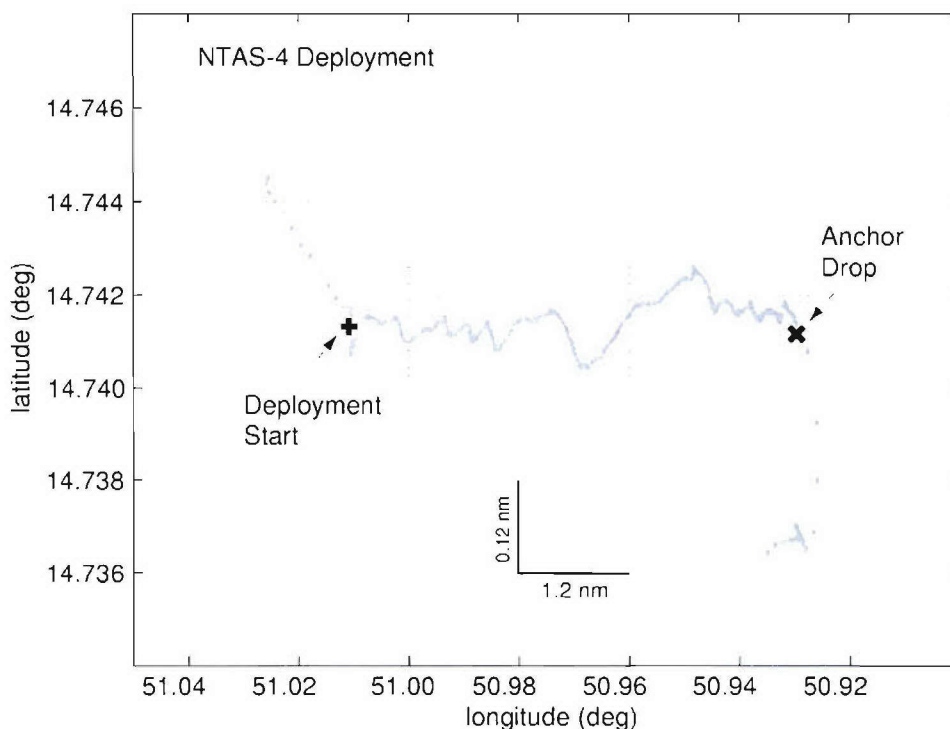


Figure 25. Ship track during NTAS-4 deployment. The period shown includes the deployment start (+), the deployment approach, and the anchor drop (x). Dots are evenly spaced at 1 min intervals; larger dot separation indicates faster ship speed. Note that the vertical scale is exaggerated by a factor of 10 relative to the horizontal scale.

The anchor survey was done to determine the exact anchor position and allow estimation of the anchor fall-back from the drop site. Three positions about 2.5 nm away from the drop site were occupied in a triangular pattern. The *Brown's* extendable 12 kHz hull transducer was used with WHOI deck gear to range on the release. The anchor survey began at 0800 h local on 22 February and took about 2.5 hours to complete. Triangulation using the horizontal range to the anchor from the three sites gave an anchor position of 14°44.430'N, 50°56.034'W. The fall-back from the drop site was about 490 m, or 10% of the water depth.

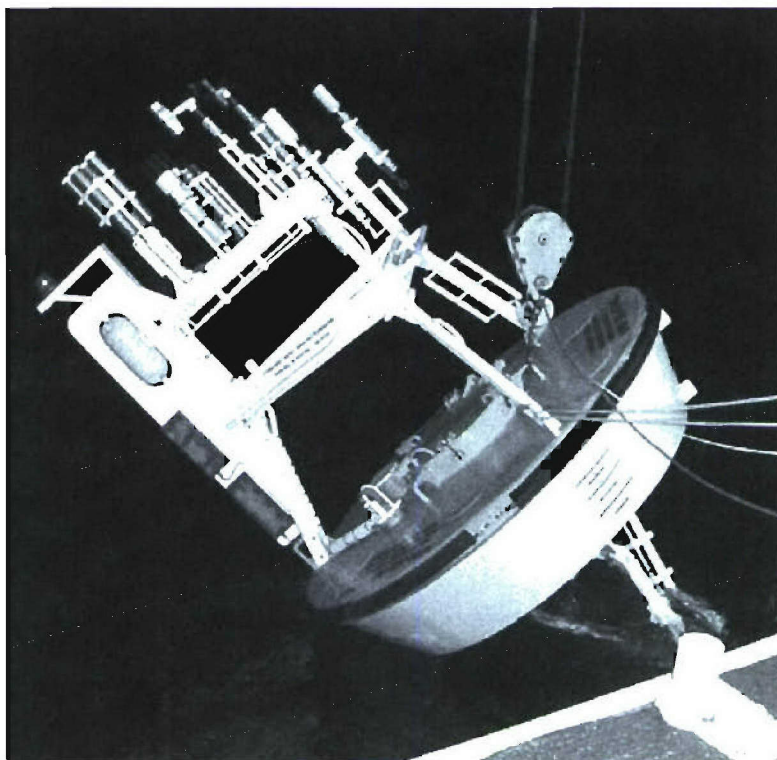


Figure 26. NTAS-4 buoy deployment.

During the intercomparison period, the ship maneuvered within a few hundred feet of the NTAS-4 buoy. Visual observations showed the tower top instrumentation intact and the buoy riding smoothly with a nominal waterline about 50 cm below the buoy deck.

6. Meteorological Intercomparisons

a. Overview

In order to assess the performance of the buoy meteorological systems, the cruise plan called for deploying the NTAS-4 mooring first, collecting buoy intercomparison data for both buoys by “shuttling” the ship between them, and then recovering the NTAS-3 mooring. However, since the NTAS-3 buoy had already been recovered after going adrift, the plan was modified to simply deploy the NTAS-4 mooring and perform the intercomparison with the ship standing-off next to the buoy. An ad-hoc intercomparison with the NTAS-3 buoy was obtained by comparing ship and buoy observations during a 7 h period on 19 February as the (drifting) buoy was approached.

During the intercomparison periods, hourly ASIMET data were obtained from the buoys by intercepting the Argos PTT transmissions with Alpha-Omega satellite uplink receivers. Whip antennas were mounted on the port and starboard rails of the 02 deck,

forward of the pilothouse. Previous experience had shown obtaining consistent receptions from both PTTs on a given buoy required that the ship stand-off at a distance of 0.25-0.5 nm downwind of the buoy. CTD casts were done in the vicinity of the NTAS-4 buoy every 4 h during the intercomparison period (see Sec. 6), during which the ship was out of range of the buoy transmissions. However, since the ASIMET logger PTTs transmit 6 h of buffered data each hour, no meteorological data were lost.

The *Brown* was outfitted with an IMET system, with sensors for barometric pressure (BP), air temperature (AT), sea surface temperature (SST), sea surface conductivity (SSC), relative humidity (RH), wind speed (WSPD), wind direction (WDIR), shortwave radiation (SWR), longwave radiation (LWR), and precipitation (PRC). Standard navigation data (GPS position, course over ground, and speed over ground) and depth from the 12-kHz echo sounder were also available. These shipboard data were logged at 1-min intervals by the Scientific Computer System (SCS) and saved as ASCII files. The 1-min data files were accessed over the network and archived on a laptop computer. These data were then averaged to 1 h for comparison with the buoys. Four of the *Brown* IMET modules were located on the bow mast: BP at 15.6 m, and WND, HRH and PRC at 14 m above the waterline. SWR and LWR modules were located on the 02 deck at a height of 10 m. The ship's BP sensor was not operating during the cruise, and was replaced by the spare ASIMET BPR module (SN 204) mounted on the 02 deck at a height of approximately 10 m. There were two sources of SST data. Both systems measured water from the sea-chest, located at a depth of 5.6 m. The IMET SST was magnetically attached to the hull inside the sea-chest, whereas the thermosalinograph (TSG) measured seawater that had been pumped from the sea-chest to the lab (the TSG also provided sea surface salinity data). The IMET SST was consistently about 0.5°C higher than the TSG sensor, a similar offset to that seen on the 2002 cruise (Plueddemann et al., 2002). The IMET SST was considered suspect, and the TSG SST was used in the comparisons.

b. NTAS-3 vs. *Ron Brown*

The ad-hoc NTAS-3 intercomparison period started at 1000 h UTC on 19 February with the ship about 120 km (65 nm) from the buoy. Note that Argos transmissions could not be received from the ship at this distance; the comparison was done after the cruise by retrieving Argos data transmitted to a WHOI workstation. Since the ship was closing on the buoy during the observation period (Fig. 27), spatial variability was reflected in the results. The buoy systems were identified by the ASIMET logger number (L03 and L06; see Table 2 in Plueddemann et al., 2003). The results of the comparison are shown in Figures 28-32. The NTAS-3 sensor pairs showed good agreement (differences between like sensors were within the expected short-term accuracy; Table 4) with the exception of RH, SWR, and LWR. Examination of the buoy data in conjunction with the shipboard meteorology provided further understanding of these discrepancies, as described below.

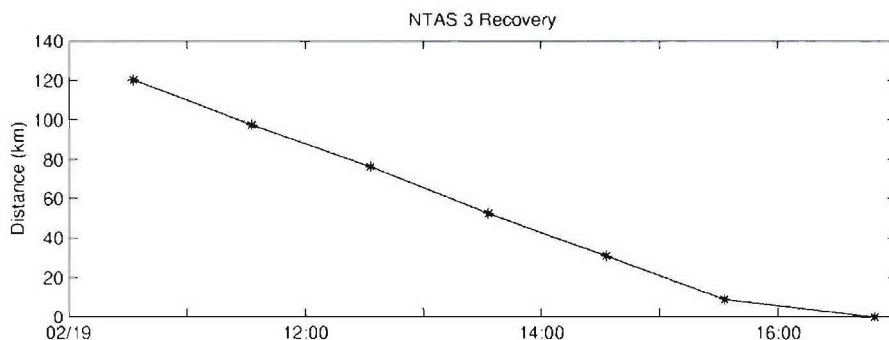


Figure 27. Distance from the NTAS-3 buoy during the ad-hoc intercomparison period.

AT (Fig. 28) was one of two buoy variables (SSC was the other) that did not converge towards the ship value as the buoy was approached. The last two hours of the comparison, with the buoy within 10 km of the ship, show buoy AT about 0.4°C above the ship. It was not clear whether this offset was attributable to calibration problems with buoy and/or ship systems or to real vertical differences in AT, but it is notable that the freshly calibrated NTAS-4 buoy also showed AT about 0.4°C higher than the ship (Fig. 33). Although the mean RH difference of 2% was within the short-term accuracy specification, this appeared to be the result of a persistent bias ($L03 > L06$) rather than short-term variability. As the buoy was approached, buoy RH converged to within 2% of the ship RH, with L06 very close to the shipboard value, and L03 about 2% high.

Buoy BP values (Fig. 29) were within 1 mb of the ship-mounted module after correction for the height difference between them. The PRC level was near zero for the ship, and 9 and 17 mm for L06 and L03, respectively. Note that for PRC it is the rate of change of level (zero during this period) that is meaningful – constant offsets are not of concern.

Shipboard SST and SSC (Fig. 30) showed much more variability than the buoy sensor pair. As the buoy was approached, SST values converged to within 0.03°C , which was considered excellent agreement. Thus, the discrepancy between buoy and shipboard SST during the approach was attributed to spatial variability. Interestingly, SSC values did not appear to converge as the buoy was approached. However, it is notable that the magnitude of the difference ($\sim 0.01 \text{ S/m}$) is near the expected accuracy throughout.

The mean difference between buoy SWR sensors was 60 W/m^2 (Fig. 31). This is most likely the result of logger clock drift, which can result in substantial SWR differences on short time scales. There is also evidence of a low bias of the buoy SWR relative to the ship. A similar bias was found between the freshly calibrated NTAS-4 sensors and the ship (Fig. 36). The mean difference between LWR sensors was 18 W/m^2 , substantially larger than the expected short-term error. The sense of the LWR bias ($L03 > L06$) was the same, and the magnitude comparable to that observed during the post-deployment intercomparison period (Plueddemann et al., 2003). Thus, it appeared that while suffering a calibration shift prior to deployment (which has plagued this generation of LWR modules), calibration during the deployment was consistent.

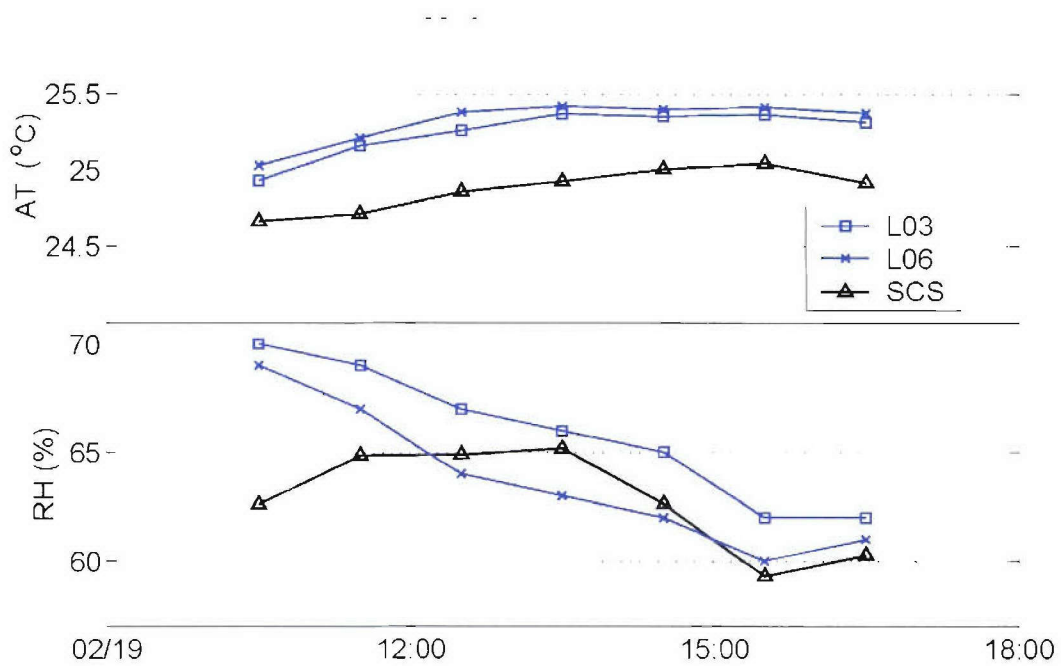


Figure 28. Air temperature (AT, upper) and relative humidity (RH, lower) for the NTAS-3 buoy systems (L03, o and L06, +) and the *Brown* (x) during the intercomparison period.

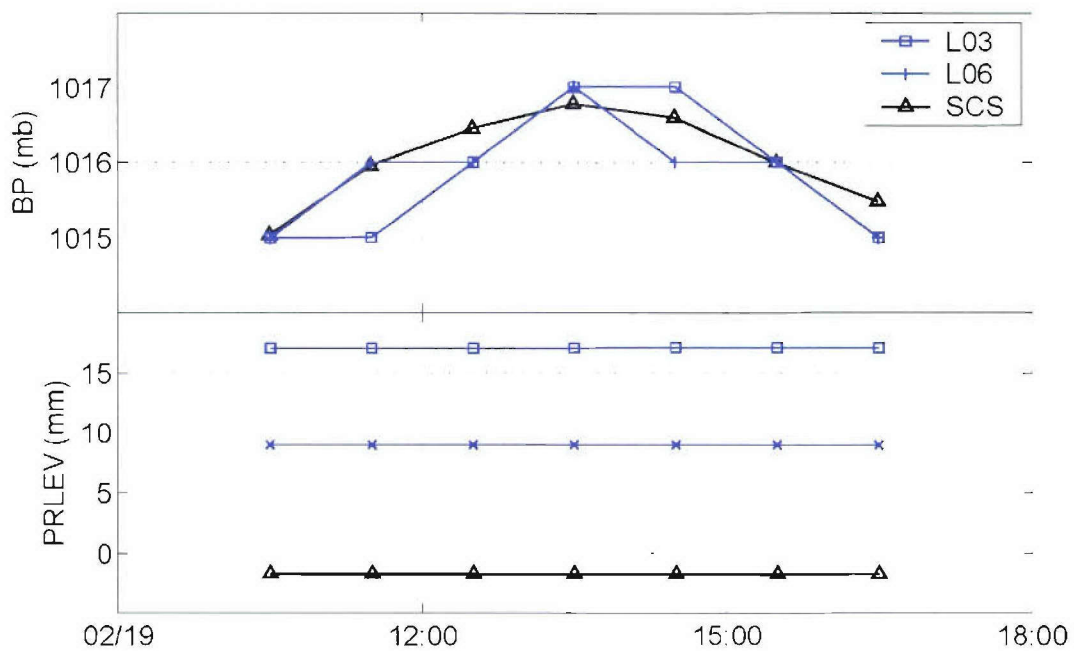


Figure 29. Barometric pressure (BP, upper) and precipitation level (PRLEV, lower) for the NTAS-3 buoy systems and the *Brown* during the intercomparison period.

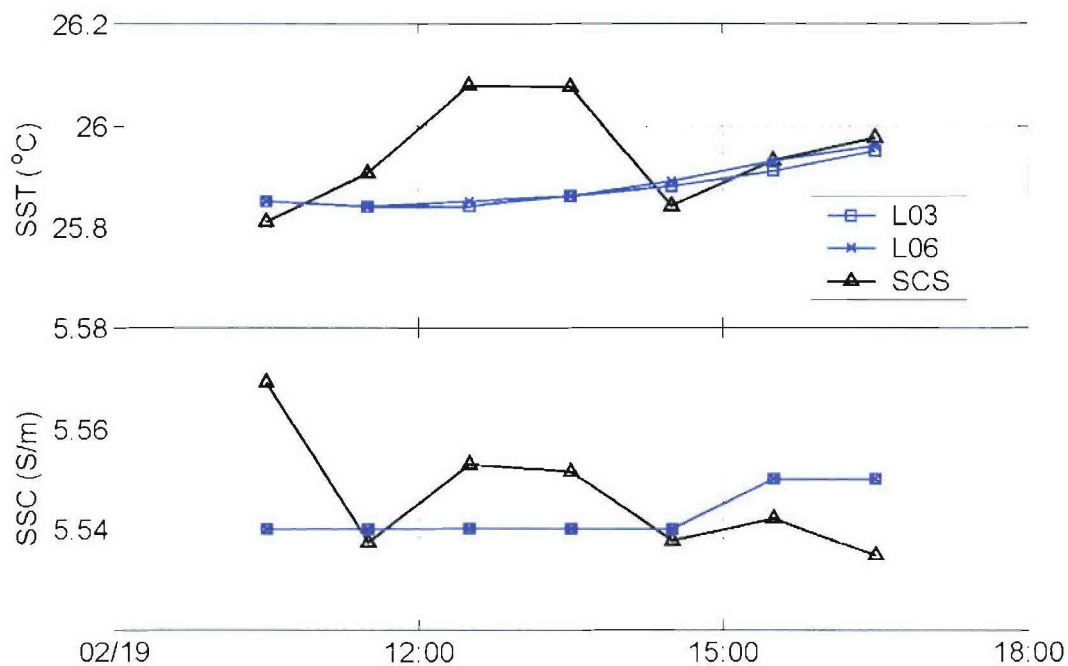


Figure 30. Sea surface temperature (SST, upper) and conductivity (SSC, lower) for the NTAS-3 buoy systems and the *Brown* during the intercomparison period.

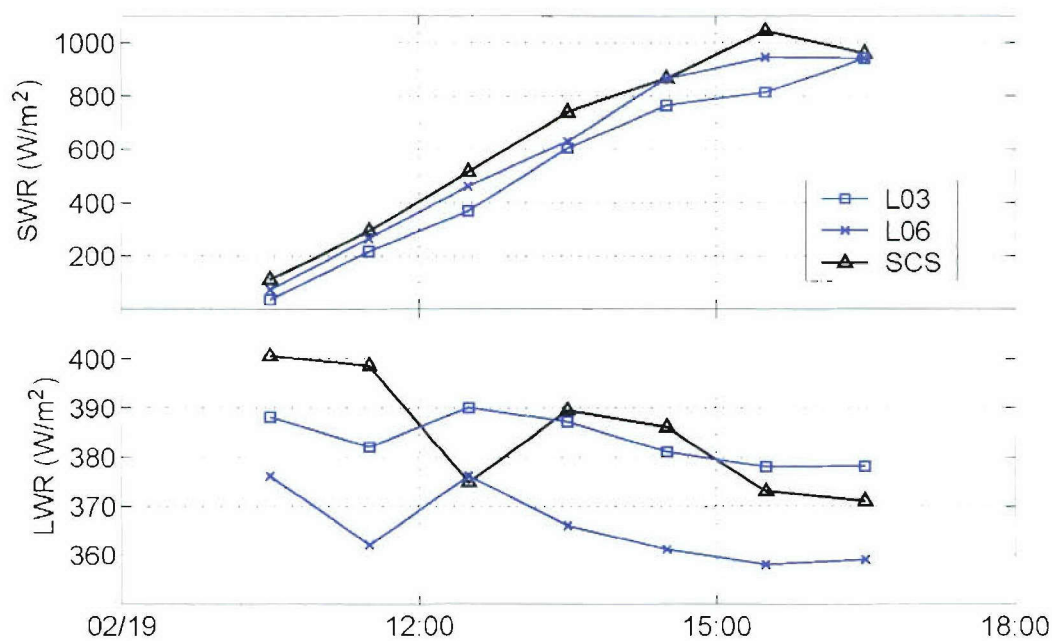


Figure 31. Shortwave (SWR, upper) and longwave (LWR, lower) radiation for the NTAS-3 buoy systems and the *Brown* during the intercomparison period.

Buoy WSPD values were within 0.1 m/s of each other and 0.5 m/s of the ship during the latter part of the approach (Fig. 32). Buoy WDIR values were within about 5° of each other and 15-20° further clockwise than the ship. Considering the potential for flow distortion around the ship's structure, this was considered reasonable agreement.

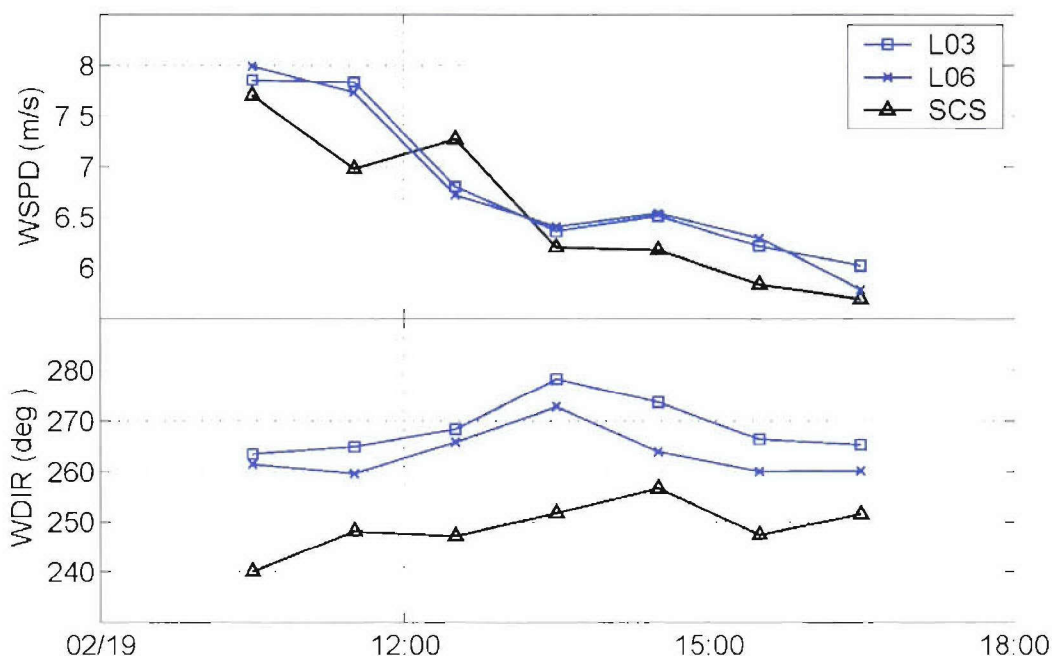


Figure 32. Wind speed (WSPD, upper) and wind direction (WDIR, lower) for the NTAS-3 buoy systems and the *Brown* during the intercomparison period.

c. NTAS-4 vs. *Ron Brown*

The NTAS-4 intercomparison started at 0400 h UTC on 21 Feb after the buoy had settled out from deployment. Operations continued until 1100 h UTC on 22 February, a total duration of 31 h. The buoy systems were identified by their ASIMET logger number (L09 and L10; see Table 5). The results of the comparison are shown in Figures 33-37. The NTAS-4 sensor pairs showed good agreement (differences between like sensors were within the expected short-term accuracy; Table 4) with the exception of LWR. Examination of the buoy data in conjunction with the shipboard meteorology provided further observations about system performance, as described below.

AT (Fig. 33) was one of two variables (SWR was the other) that were self-consistent on the buoy, yet showed a difference relative to the ship that was well out of the accuracy tolerance. The buoy AT was consistently 0.4°C higher than the ship. It seemed unlikely that both NTAS-4 sensors had suffered nearly identical calibration shifts since the pre-deployment testing and that the NTAS-3 sensors would have suffered similar shifts (Fig. 28). In addition, despite the potential for real differences in AT due to flow over the ship and the height difference between ship and buoy, previous comparisons had achieved AT agreement within 0.1-0.2°C (Plueddemann et al., 2001;

2002; 2003). Thus, the shipboard AT sensor may have been reading low by 0.2–0.4°C. Careful examination of the daytime vs. nighttime differences between buoy and ship AT suggested a modest (0.15°C.) daytime heating effect on the buoy. Both buoy RH values were in excellent agreement with the ship ($\pm 1\%$), indicating that the L03 RH from the NTAS-3 buoy was probably biased high (Fig. 28).

Buoy BP values (Fig. 34) were within 1 mb of the ship-mounted module after correction for the height difference between them. The PRC level was near zero for the ship, and near 22 mm for the buoy sensors. Note that for PRC it is the rate of change of level (zero during this period) that is meaningful — constant offsets are not of concern.

Buoy SST and SSC (Fig. 35) showed good agreement with the ship, within about 0.04°C and 0.01 S/m, respectively.

The buoy SWR sensors showed differences of 40–70 W/m² during midday (Fig. 36). Both the absolute difference and the difference as a percentage of the ambient SWR level (about 6%) were larger than expected for properly calibrated SWR sensors. Since both NTAS-3 and NTAS-4 values were lower than the ship, a consistent explanation would be a high bias of about 5% for the ship's SWR. The mean difference between buoy LWR sensors was 15 W/m², with (L09 > L10). The L09 value was within 4 W/m² of the ship, while the L10 value was 11 W/m² higher. Since this generation of buoy LWR modules was known to be susceptible to calibration shifts, it was assumed that L10 had suffered a positive shift of about 10 W/m² prior to deployment. This was consistent with expectations from the WHOI evaluation and from pre-cruise LWR testing (Sec 2b).

Buoy WSPD values were within 0.1 m/s of each other and about 0.2 m/s of the ship (Fig. 37). Buoy WDIR values were within about 8° of each other and 2–10° further clockwise than the ship. Considering the potential for flow distortion around the ship's structure, this was considered good agreement.

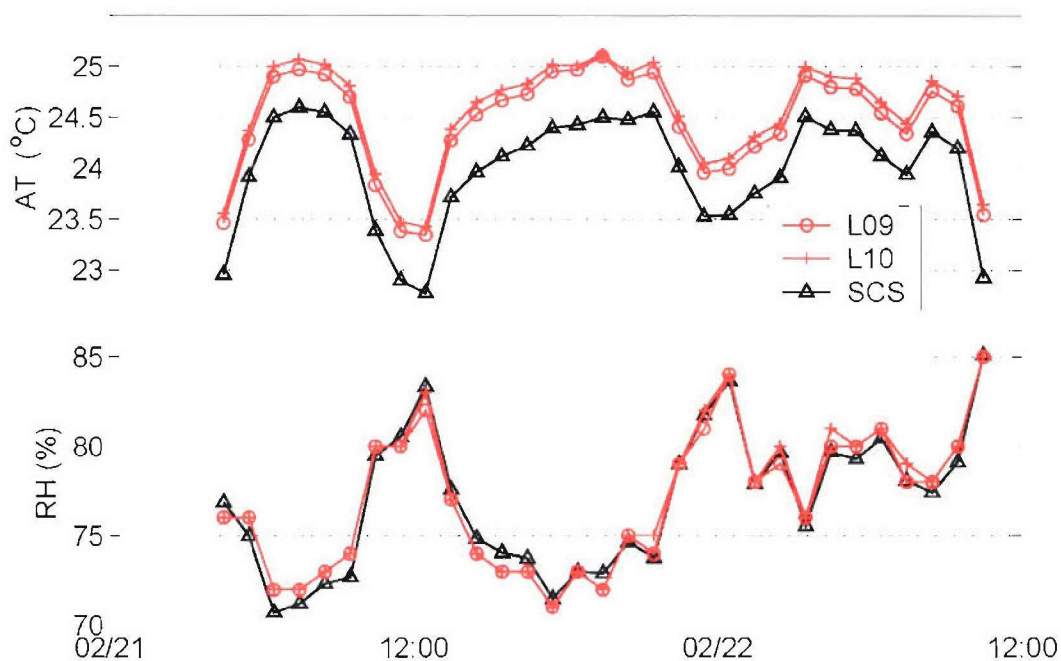


Figure 33. Air temperature (AT, upper) and relative humidity (RH, lower) for the NTAS-4 buoy systems (L09, o and L10, +) and the *Brown* (x) during the intercomparison period.

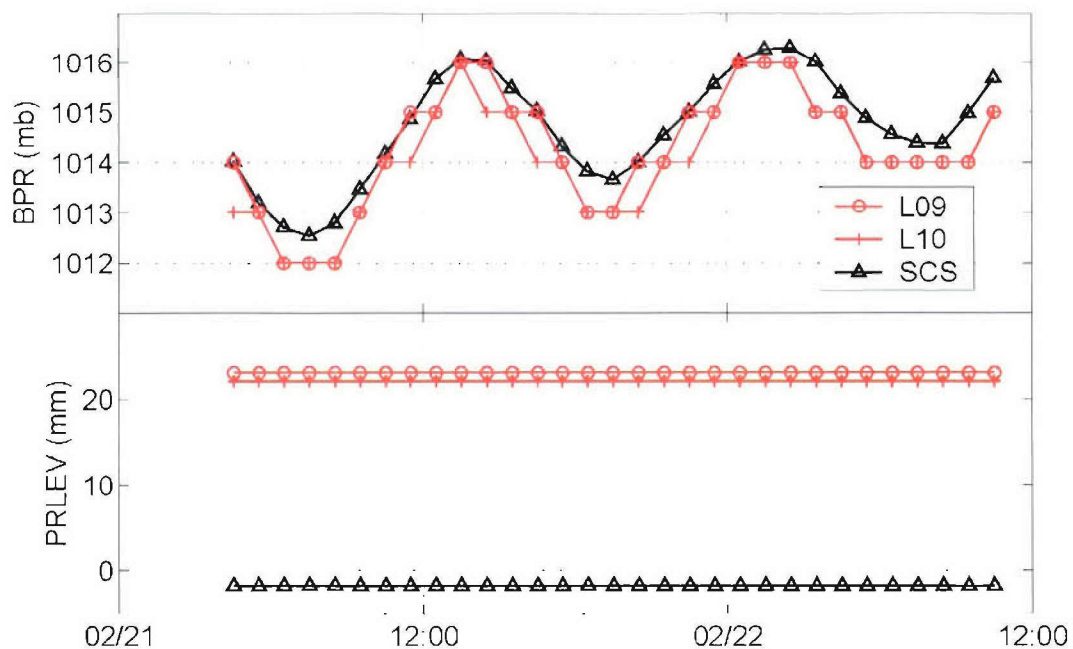


Figure 34. Barometric pressure (BP, upper) and precipitation level (PRLEV, lower) for the NTAS-4 buoy systems and the *Brown* during the intercomparison period.

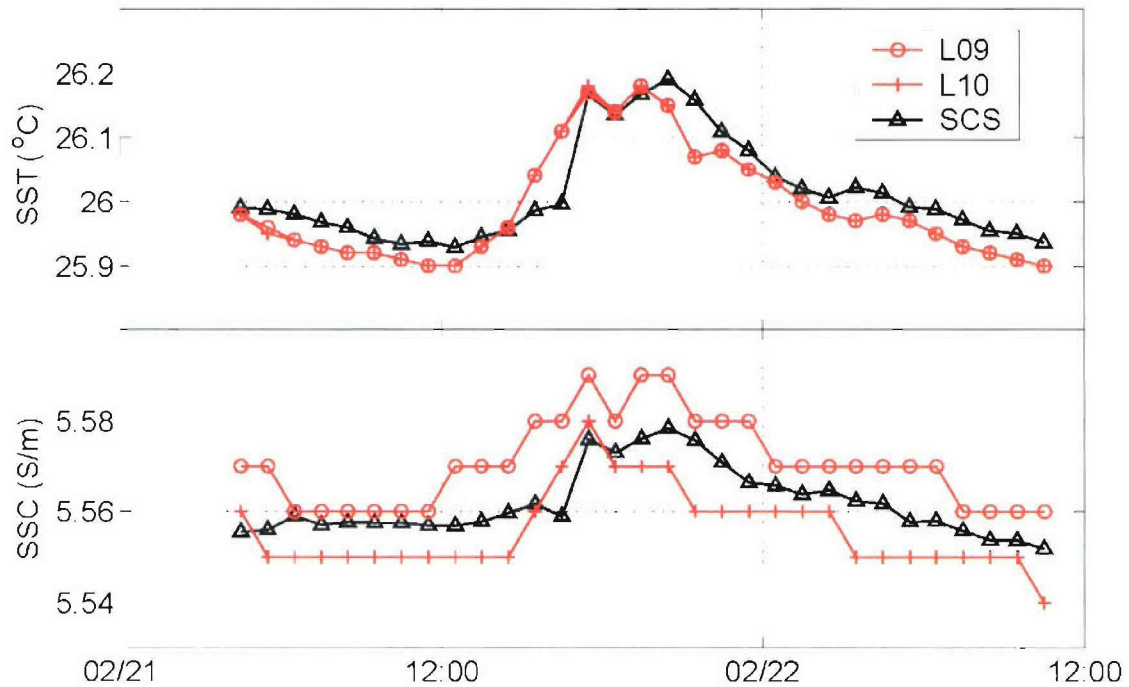


Figure 35. Sea surface temperature (SST, upper) and conductivity (SSC, lower) for the NTAS-4 buoy systems and the *Brown* during the intercomparison period.

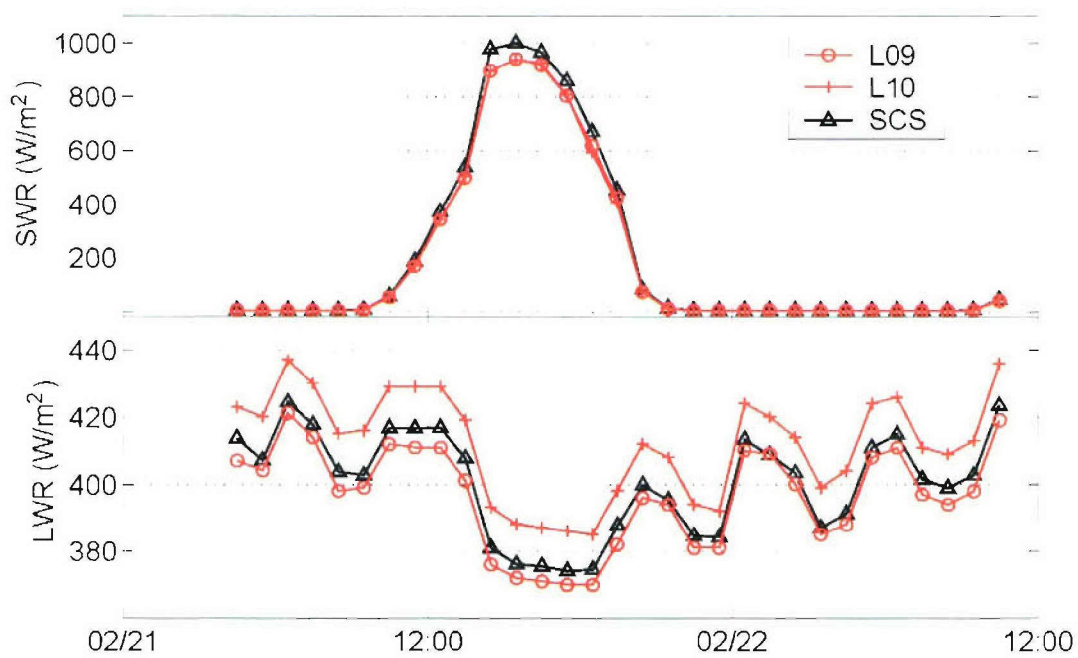


Figure 36. Shortwave (SWR, upper) and longwave (LWR, lower) radiation for the NTAS-4 buoy systems and the *Brown* during the intercomparison period.

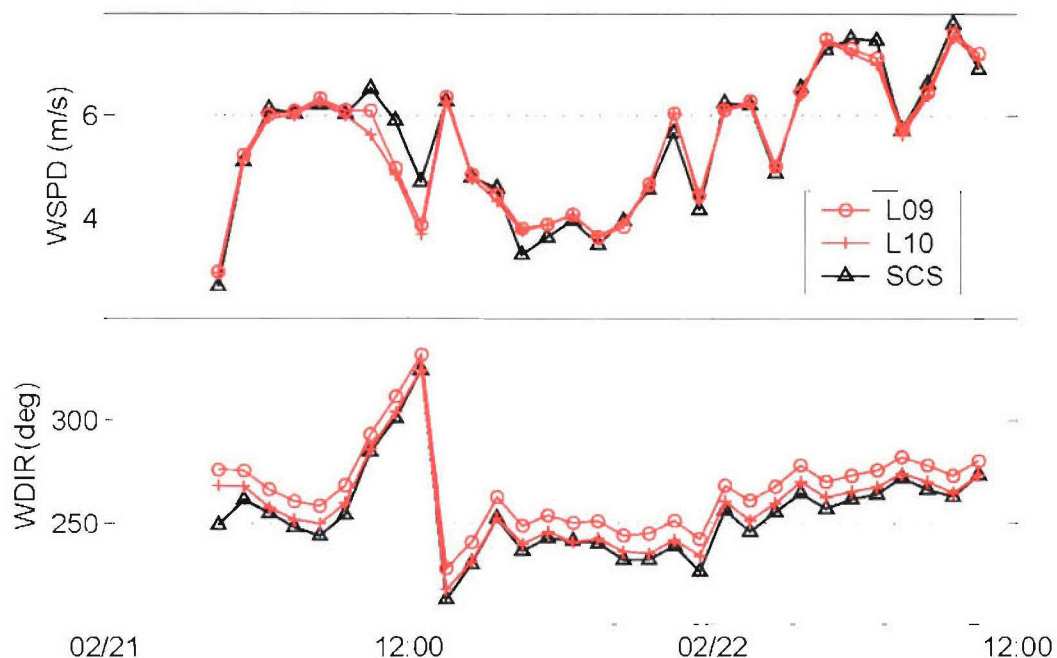


Figure 37. Wind speed (WSPD, upper) and wind direction (WDIR, lower) for the NTAS-4 buoy systems and the *Brown* during the intercomparison period.

7. CTD Casts

Five CTD casts to 500 m depth were done at 4 h intervals starting at midnight (local) on 20 February. The casts were done at a position about 0.5 nm downwind of the buoy during the meteorological intercomparison period. Each cast took about 30 min to complete. Unfortunately, several of the profiles showed salinity spiking problems that could not be completely eliminated even with careful post-processing. One of the better profiles (from Cast #3) is shown here (Fig. 38). The profiles showed a region of relatively well-mixed temperature between the surface and 70 m depth, but with three distinct salinity steps at about 10, 40 and 70 m. Temperature decreased between 80 and 150 m depth, while salinity remained relatively constant. Below 150 m both temperature and salinity decreased monotonically.

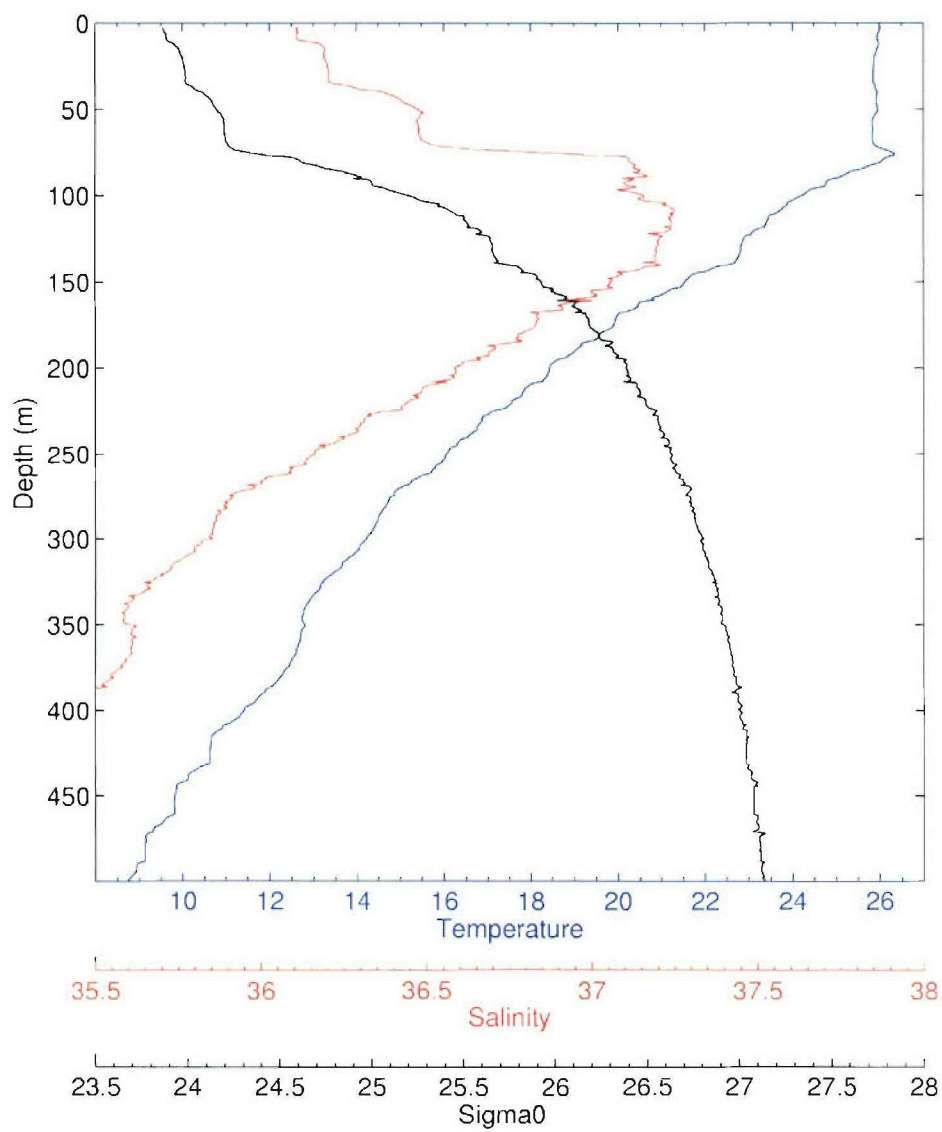


Figure 38. CTD profile from Cast #3 taken during the meteorological intercomparison period. Temperature (blue), salinity (red), and sigma-theta (black) are over plotted.

Acknowledgments

The Captain, officers and crew of the NOAA Ship *Ron Brown* were flexible in accommodating the science mission, and exhibited a high degree of professionalism throughout the cruise. The capabilities of the ship and crew were critical to the success of the mooring operations. Lara Hutto provided shore support for monitoring Argos telemetry that proved to be essential to locating the drifting NTAS-3 buoy. This project was funded by the National Oceanic and Atmospheric Administration (NOAA) through the Cooperative Institute for Climate and Ocean Research (CICOR) under Grant No. NA17RJ1223 to the Woods Hole Oceanographic Institution.

References

- Colbo, K. and R. Weller, Accuracy of the IMET sensor package, *J. Atmosph. Ocean. Technol.*, submitted.
- Hosom, D. S., R. A. Weller, R. E. Payne, and K. E. Prada, 1995. The IMET (Improved Meteorology) ship and buoy systems. *J. Atmosph. Ocean. Technol.*, **12**(3), 527–540.
- Plueddemann, A. J., N. R. Galbraith, W. M. Ostrom, G. H. Tupper, R. E. Handy, and J. M. Dunn, 2001. The Northwest Tropical Atlantic Station (NTAS): NTAS-1 mooring deployment cruise report, *Woods Hole Oceanog. Inst. Tech. Rep. WHOI-2001-07*, 55 pp.
- Plueddemann, A. J., W. M. Ostrom, N. R. Galbraith, P. R. Bouchard, G. H. Tupper, J. M. Dunn and M. A. Walsh, 2002. The Northwest Tropical Atlantic Station (NTAS): NTAS-2 mooring turnaround cruise report, *Woods Hole Oceanog. Inst. Tech. Rep. WHOI-2002-07*, 68 pp.
- Plueddemann, A. J., W. M. Ostrom, N. R. Galbraith, J. C. Smith, J. R. Ryder, J. J. Holley and M. A. Walsh, 2003. The Northwest Tropical Atlantic Station (NTAS): NTAS-3 mooring turnaround cruise report, *Woods Hole Oceanog. Inst. Tech. Rep. WHOI-2003-04*, 69 pp.
- Serra, Y.L., P. A'Hearn, H.P. Freitag and M. McPhaden, 2001. ATLAS self-siphoning rain gauge error estimates, *J. Atmosph. Ocean. Technol.*, **18**(12), 1989 – 2002.
- Smith, W.H. and D.T. Sandwell, 1997. Global sea floor topography from satellite altimetry and ship depth soundings, *Science*, **277**, 1956-1962.

Appendix 1: Cruise Participants, *Ronald H. Brown*, Cruise RB-04-01

Captain

John Wilder (CDR)

Officers

Timothy Wright (CDR)
Wade Blake (CDR, Executive Officer)
Lester Cruise (LT, Medical Officer)
Michael Hoshlyk (LT, Field Operations Officer)
Shawn Maddock (LTJG)
Jeffrey Shoup (ENS)
Silas Ayers (ENS)

Deck Department

Bruce Cowden (CB)
David Owen (BGL)
Reginald Williams (DU)
Victoria Carpenter (AB)
Michael Conway (AB)
Chris Kaanaana (OS)
James Melton (OS)

Survey Department

Johnathan Shannahoff (CST)

Electronics Department

Steve Macri (LET)

Science Party

Albert Plueddemann (Chief Scientist)
Nancy Galbraith
William Ostrom
Paul Bouchard
Brian Hogue
Brandon Wasnewski
M. Alexander Walsh
Goshka Szczodrak (RSMAS)

Appendix 2: Cruise Chronology

The *Brown* schedule indicated that the NTAS-4 cruise would depart from Charleston, SC, on 12 February 2004 and return to Bridgetown, Barbados, on 26 February. A 40' box truck and flatbed truck were loaded in Woods Hole on 3 February to arrive Charleston on 5 February (see Sec. 3), allowing 6 working days in port prior to sailing. The NTAS-4 cruise was to be the first of three science cruises, after which the ship would return to Charleston (13 April) and then perform Seabeam trials in transit to Woods Hole, arriving 3 May. Since deck use for the cruises following NTAS was relatively light, it was determined that most WHOI/UOP equipment could stay aboard to be offloaded in Woods Hole in May. The exceptions were the TSE winch, tension cart, and winding cart, which were needed back in Woods Hole before May. Arrangements were made to offload these in Charleston in April. Note that although Jeff Lord made the trip to Charleston to assist with pre-cruise operations, he did not participate on the cruise. The following summarizes activities between 4 and 25 February 2004. All times are local unless otherwise noted.

04 Feb: Ostrom and Lord depart Boston for Charleston.

05 Feb: Plueddemann, Galbraith, Bouchard, Hogue, and Wasnewski depart Boston for Charleston. The 40' box truck and flatbed truck arrive in Charleston and are unloaded directly onto the ship. The 20' ragtop container proves to be heavier than anticipated, and must be partially unloaded before being moved onto position on the port side. The buoy well insert is placed in the well and the tower top is attached to the buoy hull using the ship's crane. Science gear from the box truck is placed in the lab.

06 Feb: The TSE winch and handling gear are arranged on deck. Wiring of the buoy well and tower top begin. ASIMET modules are run through their pre-deployment checks and mounted on the tower top. Antennas for the Alpha-Omega Argos receivers are installed and the cables are run to the main lab. The buoy ASIMET system is up and running by 1300 and monitoring of Argos transmissions begins. Initial problems with expected vs. actual PTT IDs are sorted out. LWR 207 is determined to have a C51 board set, explaining its lower firmware revision (2.5) compared to the others. WND 215 is determined to have a bent prop shaft, and its wind vane is exchanged with that from WND 214.

07 Feb: Smaller deck equipment (air tuggers, deck boxes) stored in the rag-top container is unloaded and organized on deck. Overnight Argos data are evaluated and individual modules with questionable performance are checked. It is suspected that airflow blockage with the buoy on the ship is degrading the sensor comparisons. ASIMET sensor timing marks (fill/drain PRC, cover/uncover solars, salt water dunk for STC) are applied. Preparation of subsurface instrumentation and assembly of brackets begins. Tidbits and SBE-39s are running, with ice-bath

timing marks applied, by the end of the day. The Aquadopp current meter is configured and started. Stowage and tie-down of gear in the main lab begins.

- 08 Feb: Minor deck re-arrangement and main lab outfitting continue. The TSE winch is wired up, tested, and eventually found to be operating properly. Overnight Argos data show that both wind modules appear to have failed. The day's activities center around evaluation of the failed units, mounting of the spare wind module, arrangement for two additional modules to be sent from WHOI, and set up of a wind comparison test. We suspect that the failure was related to low temperatures overnight ($< 5^{\circ}\text{C}$) since all modules work at higher temperatures.
- 09 Feb: Overnight Argos data show all sensors to be functioning and in reasonable agreement (considering the flow disturbance issues on the ship). Note that it did not drop below 5°C overnight. We decide to proceed with the buoy spin in anticipation of using the two wind modules (SN 214 and 216) presently on the buoy. The buoy is lifted off the ship and moved to a nearby parking lot at about 1100, the buoy spin is completed successfully by 1430. At about 1630 the buoy is moved to the pier, facing "bow" to the wind in hopes of an overnight run without flow obstruction. Final deck preparation, including removing bulwarks, hanging blocks, and re-positioning handling gear, is done. Splicing is done to join the synthetic mooring line segments. George Schwartz arrives from URI to set up and test the LIDEX sound source. Several participants in the AEROSE and Windward Passage projects (the cruises following NTAS) arrive and begin to load their gear.
- 10 Feb: Deck arrangements are complete and the main lab is nearly ready for sea. The buoy is moved from its location on the pier by about 0830. ASIMET sensor comparisons continue using Argos data collected overnight when the buoy was on the pier with unobstructed flow towards the "bow" of the buoy. Evaluation shows all ASIMET sensors to be performing well, with differences between like sensors within the expected error tolerance. We confirm that Argos data are getting through to the WHOI web site. The bridle legs are attached to the buoy, the clevis is fitted to the bridle, and instrumentation is attached to the bridle legs. Final painting of the buoy hull is done. Loading for AEROSE and Windward Passage cruises continues in parallel with our work. Jeff Lord departs Charleston for Woods Hole. Alex Walsh arrives in Charleston.
- 11 Feb: The science party moves out of the hotel and onto the ship. ASIMET sensor comparisons continue using Argos data collected overnight, although this is of limited value since the buoy was on its side on the ship. A final coat of anti-fouling paint is applied to the buoy hull. The MicroCATs and SIS subsurface Argos transmitter are attached to the bridle legs and anti-fouling paint is applied.
- 12 Feb: The deck and lab are secured for sea in the morning. The ship's IMET sensors are mounted. The *Brown* pulls away from the pier at about 1230. Two operations must be completed before departing the harbor area: First, the RHIB, which was

Appendix 5. Evaluation of NTAS-3 Swage Failure

Crosby Group Inc., Group Laboratory, 1 July 2004

Lab Log No.: L-04-90

To: Don Conner

Subject: Evaluation of No. M502, 1/2 inch galvanized swage socket. RGA # 43325

Background: One modified 1/2-inch closed swage socket was returned to The Crosby Engineering department by Edwards, C G and company in Boston Ma. The socket had fractured in the shoulder area above the shank. The socket was submitted to the Crosby Laboratory for an evaluation.

PROCEDURE AND RESULTS

The evaluation of the returned swage socket consisted of the following:

(1) Visual/Macroscopic Examination

(2) Chemical Analysis

(3) Metallgraphic Examination

(1) Visual/Macroscopic Examination: The returned swage socket consisted of the shank section still contained on a piece of covered wire rope with a special jacket (Enclosure A, Figures 1 and 2). The eye section of the socket was not returned. The fracture had occurred in the section below the eye and approximately 3/8 of an inch above the shoulder where the shank section terminates. The fracture surface was corroded and did contain evidence of fatigue (Enclosure B). The observed beach marks on the fracture surface had progressed through more than 1/2 of the cross sectional area before the final fracture occurred. The fracture had initiated on one side below the eye and propagated perpendicular to the plane of the eye. There were no legible markings observed on the returned section of the socket. The shank section was not corroded and still contained the galvanize coating. A measurement taken on the outside diameter revealed that it had been swaged to the specified catalog maximum dimension for a 1/2 inch socket.

(2) Chemical Analysis: A chemical analysis was performed on a section from the shank of the returned swage socket. The analysis revealed that the socket had been forged from type 1035 carbon steel as required. The steel had been silicon killed and aluminum refined.

- (3) Metallographic Examination: A metallographic examination was performed on a section containing the fracture origin of the returned swage socket. The microstructure of the steel consisted of ferrite and spheroidal carbide. The socket had been "Cold Tuff" processed as required. There were no forging defects observed at the fracture origin.

Discussion: The analyses performed on the shank section from the fractured socket revealed that it had been forged from the specified steel type and had been properly heat treated. The fracture surface from the socket contained evidence of a fatigue fracture. The beach marks indicated that the final fracture had occurred when there was less than $\frac{1}{2}$ of the original cross section remaining. It appears, based on the beach marks, that the socket had been subject to a high cycle, low stress loading condition. The location of the fracture also appears to indicate that the socket was subjected to some side loading, possibly from restraint in a clevis attachment. The eye section of the socket was not returned. The pertinent markings are located on the eye section of the socket. Without a product identification code, the age of the socket could not be determined.

Prepared by:

James E. Fryar

Enclosure (A)



Figure 1. Photograph of the swage socket shank, wire rope, and jacket as it was received by the Laboratory.



Figure 2. Photograph showing the shank section of the fractured swage socket.

Enclosure (B)



Photograph showing the fracture surface from the returned ½ inch swage socket.

REPORT DOCUMENTATION PAGE	1. REPORT NO. WHOI-2006-09	2. UOP-2006-04	3. Recipient's Accession No.
4. Title and Subtitle The Northwest Tropical Atlantic Station (NTAS): NTAS-4 Mooring Turnaround Cruise Report			5. Report Date May 2006
7. Author(s) Albert J. Plueddemann, William M. Ostrom, Nancy R. Galbraith, Paul R. Bouchard, Brian P. Hoque, Brandon R. Wasnewski, M. Alexander Walsh			6.
9. Performing Organization Name and Address Woods Hole Oceanographic Institution Woods Hole, Massachusetts 02543			8. Performing Organization Rept. No.
			10. Project/Task/Work Unit No.
			11. Contract(C) or Grant(G) No. (C) NA17RJ1223 (G)
12. Sponsoring Organization Name and Address National Oceanic and Atmospheric Administration and the Cooperative Institute for Climate and Ocean Research			13. Type of Report & Period Covered Technical Report
			14.
15. Supplementary Notes This report should be cited as: Woods Hole Oceanog. Inst. Tech. Rept., WHOI-2006-09.			
16. Abstract (Limit: 200 words) The Northwest Tropical Atlantic Station (NTAS) was established to address the need for accurate air-sea flux estimates and upper ocean measurements in a region with strong sea surface temperature anomalies and the likelihood of significant local air-sea interaction on interannual to decadal timescales. The approach is to maintain a surface mooring outfitted for meteorological and oceanographic measurements at a site near 15°N, 51°W by successive mooring turnarounds. These observations will be used to investigate air-sea interaction processes related to climate variability. Deployment of the first (NTAS-1), second (NTAS-2) and third (NTAS-3) moorings were documented in previous reports (Plueddemann et al., 2001; 2002; 2003). This report documents recovery of the NTAS-3 mooring and deployment of the NTAS-4 mooring at the same site. Both moorings used 3-meter discus buoys as the surface element. These buoys were outfitted with two Air-Sea Interaction Meteorology (ASIMET) systems. Each system measures, records, and transmits via Argos satellite the surface meteorological variables necessary to compute air-sea fluxes of heat, moisture and momentum. The upper 150 m of the mooring line were outfitted with oceanographic sensors for the measurement of temperature and velocity. The mooring turnaround was done on the NOAA ship <i>Ronald H. Brown</i> , Cruise RB-04-01, by the Upper Ocean Processes Group of the Woods Hole Oceanographic Institution. The cruise took place between 12 and 25 February 2004. The NTAS-3 buoy was found adrift and recovered on 19 February at 14°53.7'N, 51°22.8'W. Deployment of the NTAS-4 mooring was on 21 February at approximately 14°44.4'N, 50°56.0'W in 5038 m of water. A 30-hour intercomparison period followed, after which dragging operations to recover the lower portion of the NTAS-3 mooring commenced. This report describes these operations, as well as other work done on the cruise and some of the pre-cruise buoy preparations.			
17. Document Analysis a. Descriptors air-sea interaction tropical Atlantic moored instrumentation b. Identifiers/Open-Ended Terms c. COSATI Field/Group			
18. Availability Statement Approved for public release; distribution unlimited.		19. Security Class (This Report) UNCLASSIFIED	21. No. of Pages 73
		20. Security Class (This Page)	22. Price